

REVIEW ARTICLE

Interplay between magnetism and superconductivity in iron-chalcogenide superconductors: crystal growth and characterizations

Jinsheng Wen^{1,2,3}, Guangyong Xu^{2,3}, Genda Gu²,
J. M. Tranquada² and R. J. Birgeneau^{1,3}

¹Physics Department, University of California, Berkeley, California 94720, USA

²Condensed Matter Physics and Materials Science Department, Brookhaven National Laboratory, Upton, New York 11973, USA

³Materials Science Division, Lawrence Berkeley National Laboratory, Berkeley, California 94720, USA

E-mail: jinshengwen@berkeley.edu, jtran@bnl.gov

Abstract. In this review, we present a summary of results on single crystal growth of two types of iron-chalcogenide superconductors, $\text{Fe}_{1+y}\text{Te}_{1-x}\text{Se}_x$ (11), and $A_x\text{Fe}_{2-y}\text{Se}_2$ ($A = \text{K, Rb, Cs, Tl, Tl/K, Tl/Rb}$), using Bridgman, zone-melting, vapor self-transport, and flux techniques. The superconducting and magnetic properties (the latter gained mainly from neutron scattering measurements) of these materials are reviewed to demonstrate the connection between magnetism and superconductivity. It will be shown that for the 11 system, while static magnetic order around the reciprocal lattice position $(0.5, 0)$ competes with superconductivity, spin excitations centered around $(0.5, 0.5)$ are closely coupled to the materials' superconductivity; this is made evident by the strong correlation between the spectral weight around $(0.5, 0.5)$ and the superconducting volume fraction. The observation of a spin resonance below the superconducting temperature, T_c , and the magnetic-field dependence of the resonance, emphasize the close interplay between spin excitations and superconductivity, similar to cuprate superconductors. In $A_x\text{Fe}_{2-y}\text{Se}_2$, superconductivity with $T_c \sim 30$ K borders an antiferromagnetic insulating phase; this is closer to the behavior observed in the cuprates but differs from that in other iron-based superconductors.

Contents

1	Introduction	3
2	Crystal growth	5
2.1	Bridgman method	5
2.2	Optical zone-melting technique	8
2.3	Vapor self-transport and flux method	10
2.4	Remaining challenges	10

3	Superconductivity in iron chalcogenides	11
3.1	Superconductivity in the 11 system	11
3.2	Pressure study on the 11 system	14
3.3	Doping with 3 <i>d</i> transition metals into $\text{Fe}_{1+y}\text{Te}_{1-x}\text{Se}_x$	15
3.4	Superconductivity in $A_x\text{Fe}_{2-y}\text{Se}_2$ ($A = \text{K, Rb, Cs, Tl, Tl/K, Tl/Rb}$) . . .	16
3.5	Summary	19
4	Magnetic correlations	19
4.1	Magnetic order	19
4.1.1	$\text{Fe}_{1+y}\text{Te}_{1-x}\text{Se}_x$ system	19
4.1.2	$A_x\text{Fe}_{2-y}\text{Se}_2$ materials	21
4.2	Spin excitations in $\text{Fe}_{1+y}\text{Te}_{1-x}\text{Se}_x$	22
4.2.1	Spin dynamics near (0.5, 0.5)	22
4.2.2	Doping dependence	25
4.3	Summary	26
5	Conclusions	27
6	Acknowledgements	28

1. Introduction

A superconducting material can conduct electric current with zero-energy loss due to the absence of electrical resistance below its superconducting transition temperature T_c ; such behavior is clearly of great practical use [1]. On the theoretical side, superconductivity was initially understood with the many-body theory developed by Bardeen, Cooper, and Schrieffer, (BCS theory) [2]; these authors explained the phenomenon of superconductivity on the basis of electron pairs whose interaction is mediated by electron-phonon coupling. In the 1980s, high-temperature superconductivity was discovered in lamellar copper-oxide materials whose T_c can be above liquid-nitrogen temperature [3, 4]. Here, the electron-phonon coupling as proposed in BCS theory is not sufficient to induce superconductivity at such high temperatures [5, 6]. In these cuprate superconducting materials, superconductivity develops from electronically doping an antiferromagnetic Mott insulating phase with carriers [5–9]. It is thus hoped that one may eventually understand the high- T_c superconductivity in terms of the interplay between magnetism and superconductivity.

Research on high- T_c superconductivity turned in a new direction in the year 2008 with the discovery of iron-pnictide superconductors [10, 11]. The initial excitement came with the discovery by Hosono’s group of superconductivity in $\text{LaFeAsO}_{1-x}\text{F}_x$ (labeled 1111, based on the elemental ratios in the chemical formula of the parent material) with $T_c = 26$ K [11], following an earlier report by the same group of superconductivity in $\text{LaFePO}_{1-x}\text{F}_x$ with $T_c \sim 5$ K [10]. The T_c was soon raised to 43 K, either by replacing La with Sm ($\text{SmFeAsO}_{1-x}\text{F}_x$) [12], or by applying pressure [13]. Several 1111 superconductors with $T_c > 50$ K have been successively reported [14–17], and the current record is 56 K in $\text{Gd}_{1-x}\text{Th}_x\text{FeAsO}$ [17]. Besides the 1111 system, four other families of iron-based superconductors have been discovered, typified by BaFe_2As_2 (122) [18–21], LiFeAs (111) [22–28], $\text{Fe}_{1+y}\text{Te}_{1-x}\text{Se}_x$ (11) [29–33], and $\text{Sr}_2\text{PO}_3\text{FePn}$ (21311) [34, 35]. Their crystal structures (figure 1) are all tetragonal at room temperature, but the 122 family crystallizes in the $I4/mmm$ space group, while the space group is $P4/nmm$ for the others [10, 26, 36–39]. One important common feature is that they are all layered structures, as in the cuprates [5–9].

Extensive research has been carried out to study the magnetic correlations. It is now well established for these materials that long-range antiferromagnetic order is suppressed with doping, while superconductivity appears above a certain doping level [37–58]. While there are a few cases where superconductivity appears suddenly after magnetic order disappears [47], it is more commonly found that magnetic order, either short- or long-ranged, coexists in some fashion with superconductivity over a finite range of doping [46, 48–52, 54, 56]. The observations that superconductivity develops concomitantly with the suppression of antiferromagnetic order in many iron-based superconductors [40, 56, 59, 60], a behaviour similar to that in cuprates [5–9, 61], suggest that there could also be a similar connection with the superconductivity. Conceptually, the simplest possibility would involve having the magnetic excitations replace phonons

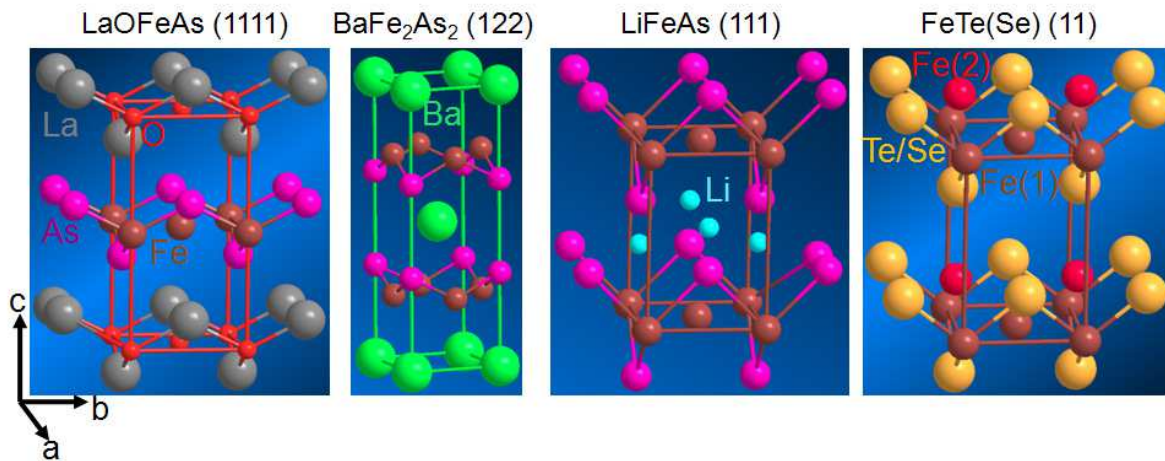


Figure 1. Schematic crystal structures for the 1111, 122, 111 and 11 type iron-based superconductors.

in the electron pairing interaction, and in the iron-based superconductors the finite momentum of the antiferromagnetic fluctuations is proposed to facilitate interband pairing [62–68]. Of course, the role of the magnetic correlations could depend on the nature of the magnetism, which continues to be a subject of intense investigation [69–76]. Furthermore, four or five Fe $3d$ orbitals are involved in the multiple bands that cross the Fermi energy, and excitations among these orbitals have also been proposed as possible contributors to the pairing mechanism [77]. In any case, the magnetic excitations respond strongly to the superconductivity: the low-energy fluctuations are gapped, and the spectral weight moves into a “resonance” peak above the gap; the resonance peak has been observed in a number of iron-based superconductors [78–86]. Obviously, the iron-based superconductors provide new opportunities to address the long-standing challenge of high- T_c superconductivity, and this has made them some of the most heavily studied materials in condensed matter physics over the past three years. A number of reviews are already available on these superconductors [57, 87–96].

Among the five types of iron-based superconductors, the T_c for the 11 system is the lowest [90]. However, the 11 materials are still of particular interest for a number of reasons: i) As seen from figure 1, the crystal structure is the simplest, which makes it easier to study them; ii) 11 system does not contain As, thus making it safer to handle; iii) Most importantly, high-quality, large-size single crystals can be made available for this system (with $x \leq 0.7$), as will be discussed in section 2. This is especially important for neutron scattering experiments because, although neutrons represent a powerful probe of magnetic correlations, the limitations of neutron source strength and scattering cross sections require the use of samples of considerable size ($\gtrsim 1 \text{ cm}^3$) in order to obtain reliable data.

More recently, the discovery of superconductivity in a ternary iron-chalcogenide system with the approximate formula $A_x\text{Fe}_{2-y}\text{Se}_2$ ($A = \text{K, Rb, Cs, Tl, Tl/K, Tl/Rb}$),

whose highest T_c is ~ 33 K at ambient pressure, has stimulated considerable interest [97–101]. The structure at high temperature is equivalent to that of the 122 materials, as shown in figure 1 (122).

The remainder of this paper is organized as follows: in section 2, we present the efforts on crystal growth that make many further measurements possible; in section 3, superconductivity in both the 11 and $A_x\text{Fe}_{2-y}\text{Se}_2$ systems is discussed; in section 4, the static and dynamic spin correlations obtained mainly by neutron scattering experiments are presented, followed by the conclusions in section 5.

2. Crystal growth

Fe-Se has a very complicated phase diagram [102]. The superconductivity in this system was found in the β - Fe_{1+y}Se , which has a tetragonal structure [29, 103]. A modified phase diagram [figure 2(a)] indicates that the β -phase only exists in a narrow temperature (300–440 °C) and composition window (Fe:Se= 1.01–1.03) [103]. Because there is no common phase boundary line between the liquid phase region and the Fe_{1+y}Se solid phase region in the Fe-Se phase diagram [102], it is not possible to grow a single crystal of Fe_{1+y}Se directly from Fe-Se liquid. Therefore, methods that rely on growing a crystal directly from a melt can not be used in this case. Instead, other growth methods, such as vapor self-transport growth [104] and alkali-halide-flux growth [105–107] have been reported.

In contrast, tetragonal Fe_{1+y}Te , though not superconducting, is stable in a larger temperature and composition space [figure 2(b)], and large single crystals can be grown directly from the melt, with a certain amount of excess Fe [31, 32]. It was quickly found that mixing Se with Te both optimizes T_c (at ambient pressure) and allows melt growth techniques. Indeed, to-date, large-size single crystals of $\text{Fe}_{1+y}\text{Te}_{1-x}\text{Se}_x$ with $x \leq 0.7$ have been successfully grown utilizing several standard melting techniques, including Bridgman (vertical and horizontal) [31, 32, 56, 86, 109–120], and optical zone-melting [121]. For the newly discovered $A_x\text{Fe}_{2-y}\text{Se}_2$ system, typically the Bridgman method has been employed [97–99, 122–126].

2.1. Bridgman method

In figure 3(a) and (c) we show the schematics for the vertical and horizontal versions of the Bridgman technique. An example of a synthesis scheme is as follows. To start with, the raw materials (99.999% Te, 99.999% Se, and 99.98% Fe) are weighed and mixed with the desired molar ratio, and then sealed into an evacuated, high-purity (99.995%) quartz tube. Since the tube often cracks during the cooling cycle, it is sealed inside a larger evacuated tube. The doubly-sealed materials are then put into the furnace vertically (or horizontally) for pre-melting, with the following sequence: ramp to 660 °C in 2 hrs; hold for 1 hr; ramp to 900 °C in 1 hr; hold for 1 hr; ramp to 1050 °C in 1 hr; hold for 3 hrs; shut down the furnace and cool to room temperature. The reacted materials are then crushed and double-sealed into evacuated quartz tubes for

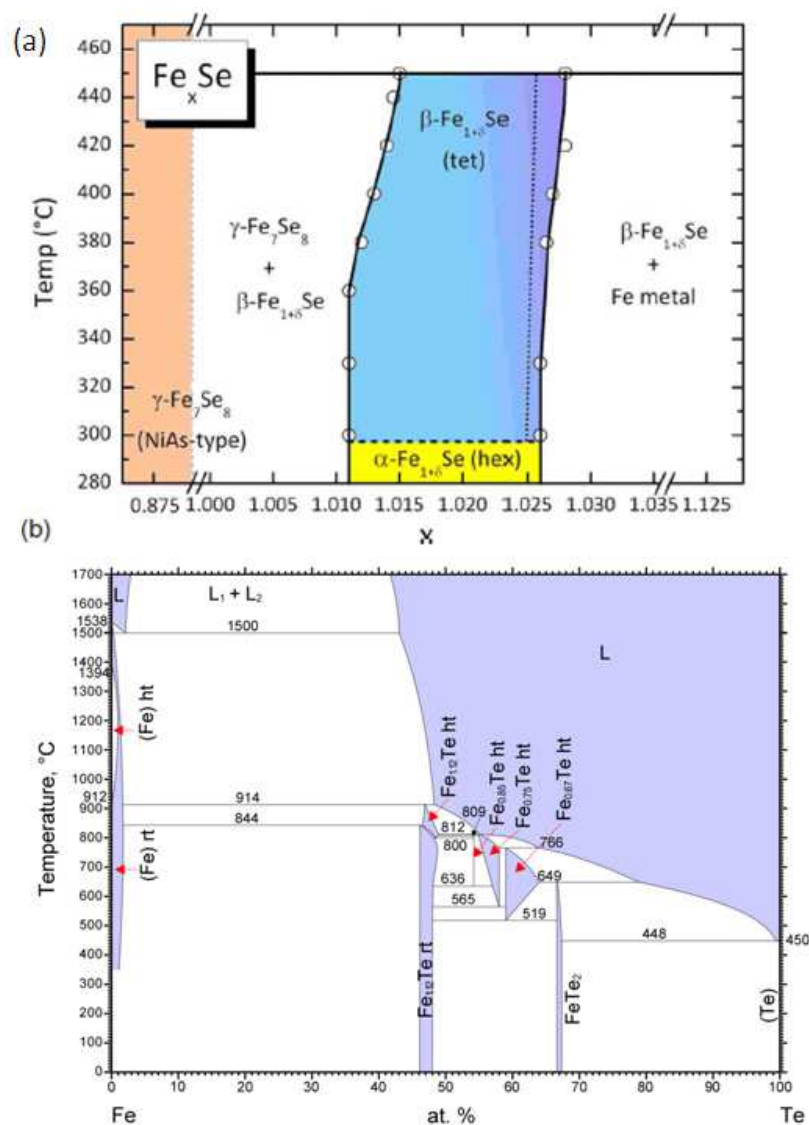


Figure 2. (a) Phase diagram for Fe-Se. Reprinted from [103]. © 2009 American Physical Society. (b) Phase diagram for Fe-Te. Reprinted from [108]. © ASM International.

the growth sequence: ramp to 660 °C in 3 hrs; hold for 1 hr; ramp to 900 °C in 2 hrs; hold for 1 hr; ramp to 1000 °C in 1 hr; hold for 12 hrs; cool to 300 °C with a cooling rate of -0.5 or -1 °C/hr; shut down the furnace and cool to room temperature. In the furnace, there should be a small temperature gradient from one end to the other (*e.g.*, at 850 °C, $\Delta T/\text{distance} \approx 5$ °C/cm) as shown in figure 3(a) and (c), which allows directional solidification of the melted liquid. (Some may choose to skip the premelting step.) By using this method, large-size (> 10 g) high-quality single crystals can be obtained for Fe_{1+y}Te_{1-x}Se_x with $x \leq 0.7$. Figure 3(b) and (d) show some of the crystals grown using vertical and horizontal Bridgman methods. The crystals can have nice mirror-like cleavage surfaces, corresponding to the *a-b* planes; however, in our

experience, such crystals have excess Fe ($y > 0$) and a reduced superconducting volume fraction. Crystals with a large superconducting volume fraction (with $y \approx 0$) tend to have a textured cleavage surface associated with slight misorientation of grains, due to strain effects that develop on cooling in the constrained cross section of a quartz tube.

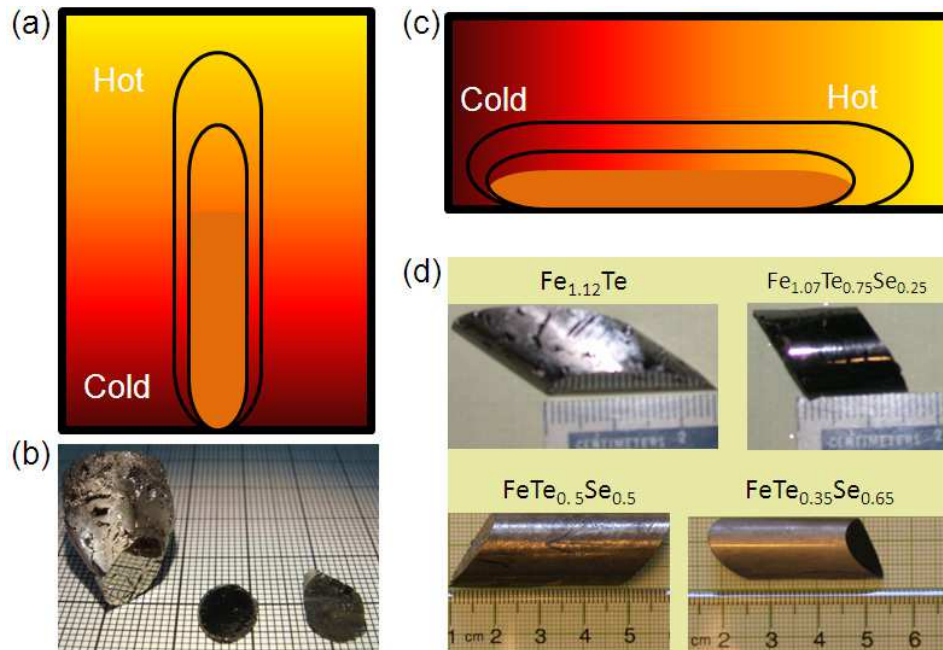


Figure 3. (a) Schematic of the vertical Bridgman growth. (b) Crystals grown using the method shown in (a). Reprinted from [31]. © 2009 American Physical Society. (c) Horizontal Bridgman growth. (d) Crystals grown using the method shown in (c) [127].

Many measurements such as resistivity, magnetization, x-ray diffraction (XRD) and neutron diffraction have been carried out to characterize such crystals [31, 32, 56, 86, 109–120]. In figure 4 we show the bulk magnetization and rocking curve for $\text{FeTe}_{0.5}\text{Se}_{0.5}$ samples. The transition width, ΔT_c , is ~ 1 K [figure 4(a)], indicating that the sample is reasonably homogeneous. From neutron diffraction measurements, we obtained a mosaic spread of 0.85° for a 9-g sample [figure 4(b)]. These demonstrate that high-quality, large-size single crystals on $\text{Fe}_{1+y}\text{Te}_{1-x}\text{Se}_x$ ($x \leq 0.7$) can be successfully grown using the Bridgman method.

To grow single crystals of $A_x\text{Fe}_{2-y}\text{Se}_2$, a similar method has been used. First, FeSe is prepared as the precursor by reacting Fe and Se in the appropriate ratio at 700°C for 4 hrs. The alkali and the precursor FeSe are loaded into an alumina crucible with the nominal composition, which was then sealed into a tube; Wang *et al.* [122] have demonstrated the benefits of using an arc-welded Ta tube. The tube is then put into an evacuated quartz tube and sealed. A typical growth sequence is: ramp to 1050°C in 15 hrs; hold for 4 hrs; cool to 750°C at a rate of -1 to -3°C/hr ; shut down the furnace and cool to room temperature. Large-size single crystals can be obtained using this method, and single crystal rods so-obtained are shown in figure 5. A one-step method

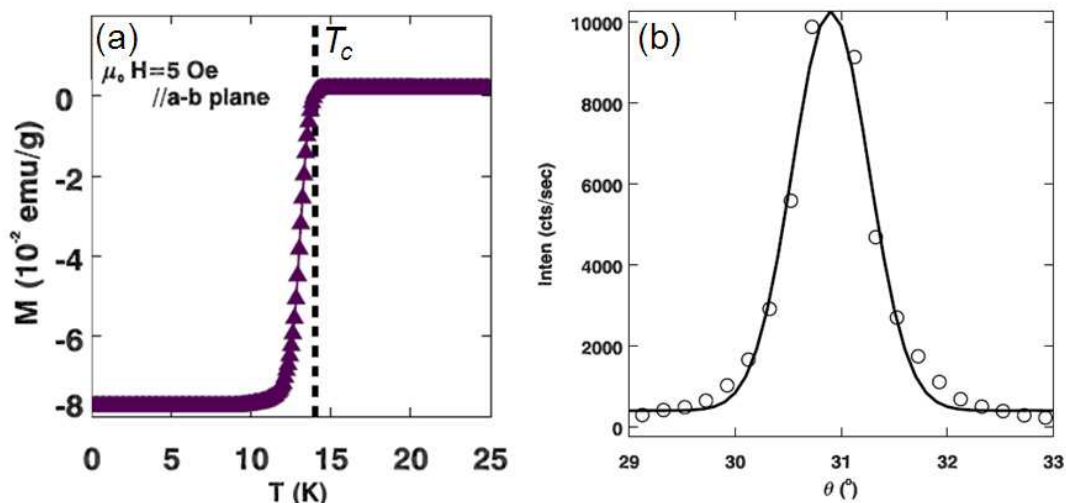


Figure 4. (a) and (b), magnetization and (110) rocking curve of $\text{FeTe}_{0.5}\text{Se}_{0.5}$ samples.

using a similar growth procedure but without first reacting Fe and Se as the precursor has also been reported [126].



Figure 5. Single crystal rods of $\text{K}_{0.8}\text{Fe}_2\text{Se}_2$ grown using the vertical Bridgman method [128].

2.2. Optical zone-melting technique

Yeh *et al.* [121] have used the optical zone-melting method to grow $\text{Fe}_{1+y}\text{Te}_{1-x}\text{Se}_x$ single crystals with x ranging from 0 to 0.7. The advantage of this technique is that it offers the possibility of visually examining the locally melted zone, as well as providing convenient control of the growth rate using the image furnace. The schematic of the setup is shown in figure 6(a). To grow single crystals, powders of 99.9% Fe, 99.9% Se, and 99.999% Te were combined with the desired stoichiometry and mixed in a ball mill for 4 hrs. The mixed powders were cold pressed into discs under 400-kg/cm^2 uniaxial pressure, and then sealed into an evacuated quartz tube. The tube was heated at 600°C for 20 hrs. The reacted bulk material was reground to fine powder and then sealed into an evacuated quartz tube. The tube was sealed into a second evacuated tube, and then loaded into an optical floating-zone furnace with two 1500-W halogen lamps installed

inside the mirrors as infrared radiation sources, as shown in figure 6(a). The ampule was rotated at a rate of 20 rpm and moved downwards at a rate of 1-2 mm/hr. The as-grown crystals are annealed with the following sequence: ramp to 700-800 °C in 7 hrs; hold for 48 hrs; cool to 420 °C in 4 hrs; hold for 30 hrs; shut down the furnace and cool to room temperature.

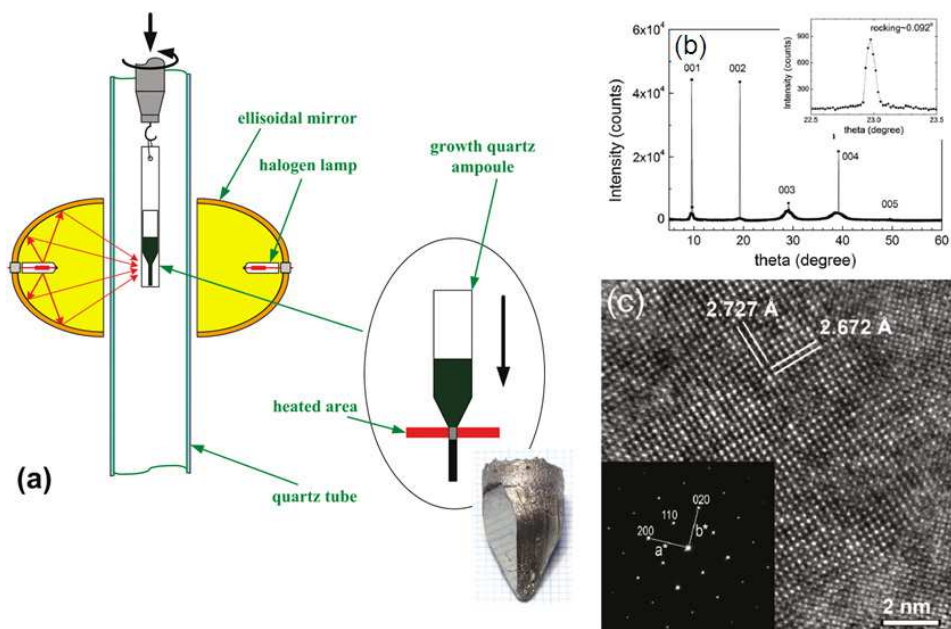


Figure 6. (a) Schematic diagram of apparatus setup of the optical zone-melting method. The inset shows an as-grown $\text{FeTe}_{0.7}\text{Se}_{0.3}$ single crystal on a 1-mm grid. The shiny surface is the a - b plane. (b) XRD pattern for an $\text{FeSe}_{0.3}\text{Te}_{0.7}$ crystal. Miller indices for the tetragonal-PbO structure are shown. The inset shows the rocking curve for the (101) peak. (c) High-resolution TEM image of an $\text{FeSe}_{0.3}\text{Te}_{0.7}$ crystal and the electron diffraction indexed with a tetragonal lattice. Reprinted from [121]. © 2009 American Chemical Society.

The inset of figure 6(a) shows an as-grown crystal for $\text{FeSe}_{0.3}\text{Te}_{0.7}$, which has an easily cleaved surface perpendicular to the c axis [121]. As shown in figure 6(b), only (00 L) peaks were found in the typical XRD pattern on a cleaved surface of the crystal, indicating that the cleaved surface corresponds to the a - b plane. In the inset of figure 6(b) it is shown that the crystal has a mosaic as small as 0.092° . The phase purity was examined by x-ray powder diffraction with powder obtained by crushing the crystals. Yeh *et al.* [121] found that all diffraction peaks of crystals with $x < 0.7$ belong to the tetragonal phase and no secondary phase was observed. High-resolution transmission electron microscopy (TEM) measurements showed that the diffraction patterns could be well indexed with a tetragonal structure, as shown in the inset of figure 6(c) [121].

2.3. Vapor self-transport and flux method

The phase diagram of Fe-Se is such that one cannot grow large crystals of the β -FeSe directly from standard melting methods; Patel *et al.* [104] used vapor self-transport as an alternative approach. They began by mixing 99.9% Fe and 99.99% Se powders with the desired molar ratio. The mixture was ground and sealed into an evacuated quartz tube. The material was then heated in a three-zone furnace with the following procedure: 1) heat the material with the temperatures for the three zones set to 700 °C (where the Fe and Se mixture is located), 900 °C, and 900 °C, respectively, for 5 days; 2) crystal nucleation is initiated by setting the temperature of all zones to 700 °C, and the temperature held constant for 5 hrs; 3) the crystals are left growing for 30 days with a temperature setting of 825 °C, 700 °C, and 825 °C, respectively; 4) the system is cooled to 400 °C rapidly, and the temperature is kept constant for 10 hrs; 5) cool to room temperature at a rate of -3 °C/min. X-ray diffraction indicated that the dominant phase in the as-grown crystal was superconducting β -Fe_{1+y}Se, with a minority of non-superconducting α -FeSe [104].

Another approach is to use an alkali-halide flux. Zhang *et al.* [105] made use of a NaCl/KCl flux. First, Fe and Se powders with the desired stoichiometry were reacted to obtain Fe_{1+y}Se polycrystalline samples. This material was mixed with NaCl/KCl flux (ratio 1:1), and the combination was ground and sealed in an evacuated quartz tube. The quartz tube was heated to 850 °C. The temperature was maintained at 850 °C for 2 hrs before cooling to 600 °C at a rate of -3 °C/hr. Finally, the furnace was cooled rapidly to room temperature. The crystals were separated from the flux by dissolving the NaCl/KCl flux in deionized water. There is also a report of using KCl(KBr) as the flux [107].

Hu *et al.* [106] have recently demonstrated an improved method, utilizing a flux of LiCl/CsCl. Refinement of synchrotron XRD data yielded a stoichiometry of Fe_{1.00(2)}Se_{1.00(3)}.

2.4. Remaining challenges

As described above, it has been demonstrated that large crystals of Fe_{1+y}Te_{1-x}Se_x with $x \leq 0.7$ can be grown from the melt; however, challenges remain in obtaining homogeneous samples [129, 130]. Hu *et al.* [130] performed scanning transmission electron microscopy (STEM) and electron energy loss spectroscopy (EELS) measurements on a series of as-grown Fe_{1+y}Te_{1-x}Se_x crystals. They found that all these samples showed nanoscale phase separation and chemical inhomogeneity of the Te/Se content. They attributed this to the presence of a miscibility gap in the phase diagram. The same conclusion was reached in an extended x-ray absorption fine-structure (EXAFS) study on Fe_{1+y}Te_{1-x}Se_x, where it was observed that the local structure differed from the average [129]. Scanning tunneling microscopy/spectroscopy (STM/STS) measurements on a FeTe_{0.55}Se_{0.45} sample also showed that there were Te- and Se-rich regions, whereas the averaged Te and Se contents were still 0.55 and 0.45,

respectively [131]. The sample inhomogeneity may account for the broad transitions in these materials [92, 121]. One way to improve crystals is to use a smaller cooling rate during the growth. For example, from our own experience, using a -1 °C/hr cooling rate yields better crystals than using -3 °C/hr. Annealing the as-grown crystals can also be useful [58, 111, 118, 121]. Vacuum annealing can make the Se/Te distribution more homogeneous, thus improving the superconducting volume fraction [111, 118]. Alternatively, it has been reported that annealing in air reduces the amount of excess iron [58], which can be important for observing bulk superconductivity in samples with large Te concentrations. Annealing in oxygen has been used to induce bulk superconductivity in the sulphide version, $\text{Fe}_{1+y}\text{Te}_{1-x}\text{S}_x$, at small x [109]. It is more challenging to grow crystals of $\text{Fe}_{1+y}\text{Te}_{1-x}\text{Se}_x$ with $x > 0.7$ [121]. So far, large crystals (on the order of 1 g) have not yet been reported in this range. Even for small crystals or polycrystalline samples of Fe_{1+y}Se , impurity phases such as α -FeSe, Fe_7Se_8 , Fe_3O_4 , and Fe are often found [104, 106], because of the complex phase diagram, as shown in figure 2(a) [102, 103]. Nevertheless, a recent study has reported the growth of phase pure and stoichiometric crystals of superconducting FeSe [106].

The major obstacle that limits the understanding of the intrinsic properties of $A_x\text{Fe}_{2-y}\text{Se}_2$ is the difficulty in preparing phase-pure superconducting samples. An initial TEM study on a superconducting sample of nominal composition $\text{KFe}_{2-y}\text{Se}_2$ ($0.2 \leq y \leq 0.3$) clearly demonstrates that there is nanoscale phase separation along the c axis—in some regions, there is Fe-vacancy ordering, while in others the vacancies are disordered [132]. In a recent ARPES study, a variety of results were interpreted in terms of the coexistence of different phases separated mesoscopically [133]. More effort on this system will be necessary in order to achieve predictable synthesis of single-phase samples.

3. Superconductivity in iron chalcogenides

3.1. Superconductivity in the 11 system

Superconductivity in the iron chalcogenides was first discovered in Fe_{1+y}Se , with zero resistance at $T = 8$ K, as shown in figure 7 [29]. The upper critical field at zero temperature, $\mu_0 H_{c2}(0)$, was estimated to be 16.3 T [29]. The composition of the superconducting phase was initially reported to be $\text{FeSe}_{0.88}$ by Hsu *et al.* [29], and a similar composition, $\text{FeSe}_{0.92}$, was identified by Margadonna *et al.* [134]; however, these powder samples showed a significant fraction of secondary phases in diffraction measurements. McQueen *et al.* [103] followed this work with a careful study of synthesis conditions and composition. They showed that synthesis from powders generally leads to problems with oxygen contamination, resulting in an overestimate of the Fe content in the sample. By using large pieces of Fe and Se as starting materials, they found that the stable composition range of Fe_{1+y}Se is $0.01 \leq y \leq 0.03$ (consistent with much earlier work on the phase diagram [102]), with $T_c = 8.5$ K at $y = 0.01$ and dropping

to zero at 0.03. Synchrotron x-ray diffraction indicated single-phase samples. As a further test, Pomjakushina *et al.* [135] prepared a series of samples with different initial compositions, and analyzed the composition by Rietveld refinement of neutron powder diffraction data, obtaining $\text{FeSe}_{0.975}$ (or $\text{Fe}_{1.025}\text{Se}$) for the superconducting phase in these multiphase samples, close to stoichiometry. Finally, there is the impurity-free single crystal of Hu *et al.* [106] that has been analyzed as stoichiometric. It seems reasonable to conclude that the superconducting composition is close to stoichiometry. To establish convincingly the nature of any defects (Fe interstitials, Se vacancies, etc.), one would need to test for diffuse scattering from a single crystal. Such measurements on Fe_{1+y}Te have revealed a clear signature of atomic displacements associated with Fe interstitials [136].

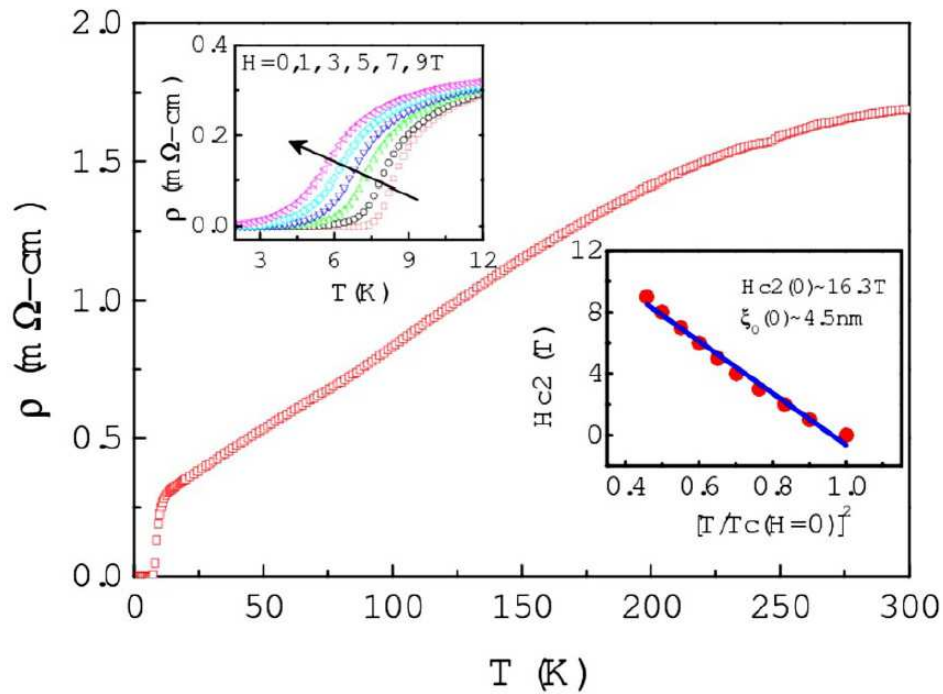


Figure 7. Temperature dependence of electrical resistivity (ρ) of $\text{Fe}_{1.14}\text{Se}$. Left inset shows resistivity *vs* temperature under different field strength below 12 K. Right inset shows the temperature dependence of the upper critical field. Reprinted from [29]. © 2008 National Academy of Sciences of the U.S.A.

At room temperature, Fe_{1+y}Se has a tetragonal PbO-type structure belonging to the $P4/nmm$ space group as shown in figure 1(11). It has an iron-based planar sublattice equivalent to that of the iron pnictides [10, 11]. On cooling below ~ 90 K, there is a structural transition to an orthorhombic phase (space group $Cmma$) [134, 135, 137], resulting in a subtle distortion of the FeSe_4 tetrahedra. The transition temperature is observed to be sensitive to composition [137].

Systematic results for the in-plane electrical resistivity of $\text{FeTe}_x\text{Se}_{1-x}$ are shown in figure 8(a) [31]. Fe_{1+y}Te is not superconducting; instead, it exhibits coincident magnetic

and structural transitions at ~ 65 K [54, 138–140]. This behaviour is similar to that of the undoped phases of the 1111 and 122 materials [38, 40–58], and it is therefore often referred to as the parent compound for the 11 system [33, 138, 139, 141, 142]. By replacing Te with Se, the structural transition temperature is gradually suppressed [140]. With 6% Se doping, a trace of superconductivity starts to appear, and coexists with the antiferromagnetic order [54]. With increasing Se content, the superconducting volume fraction improves, and T_c also becomes optimized for $x \sim 0.5$ [30, 31, 33]. Superconductivity extends all of the way to $x = 1$ in Fe_{1+y}Se , as discussed above.

Other combinations of chalcogenides are also possible. For example, one can substitute S for Se in $\text{Fe}_{1+y}\text{Se}_{1-z}\text{S}_z$. For $z = 0.2$, T_c is increased slightly, to 10 K [143]. The T_c increase is accompanied by suppression of the tetragonal-to-orthorhombic transition temperature, with the transition already absent at $z = 0.1$ [143]. For $z > 0.2$, T_c gradually decreases, with no superconductivity observed for 0.4 S [143]. Doping S into the parent compound Fe_{1+y}Te can also induce superconductivity [109, 120, 141], while suppressing the magnetic and structural transitions. The highest T_c in the $\text{Fe}_{1+y}\text{Te}_{1-z}\text{S}_z$ system is 10 K in $\text{FeTe}_{0.8}\text{S}_{0.2}$ [141].

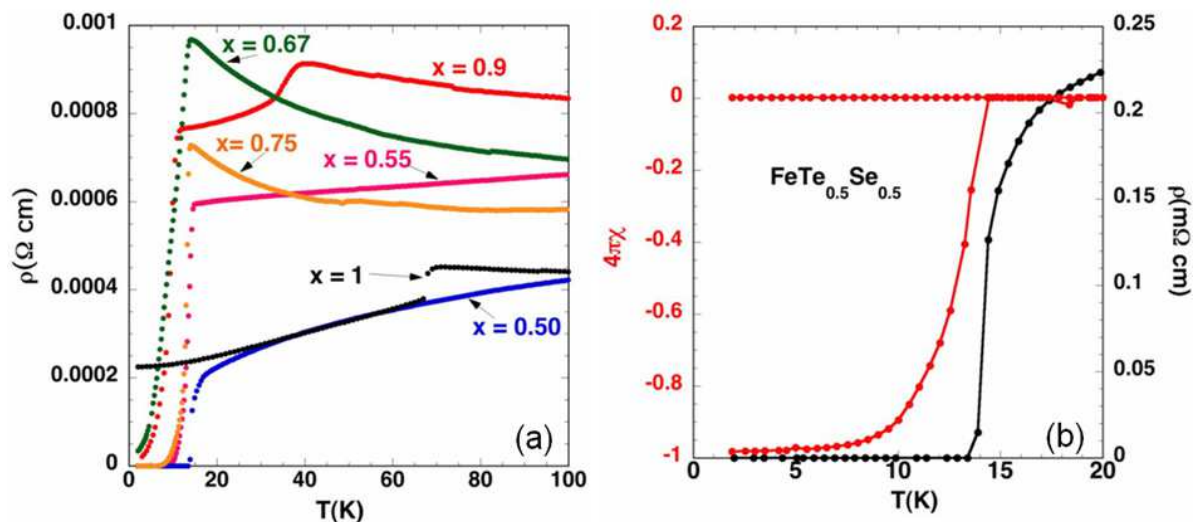


Figure 8. (a) In-plane electrical resistivity ρ as a function of temperature for $\text{FeTe}_x\text{Se}_{1-x}$. (b) Magnetic susceptibility of a $\text{FeTe}_{0.5}\text{Se}_{0.5}$ crystal measured with $\mu_0 H = 20$ Oe using zero-field cooling and field-cooling protocols. The resistivity data from the same sample are also shown on the right axis. Reprinted from [31]. © 2008 American Physical Society.

Figure 8(b) shows the magnetic susceptibility and resistivity of the optimally-doped sample, $\text{FeTe}_{0.5}\text{Se}_{0.5}$ [31]. It has a T_c of 14 K, highest in the 11 system at ambient pressure, with a superconducting volume fraction close to 100% [31, 86]. One thing to note is that in some of the thin film samples, an enhancement of T_c was observed [144, 145] (which may be related to strain effects, as pressure can enhance T_c ; see section 3.2), while in other cases the opposite effect has been reported [146, 147]. For

the optimally doped compound, the estimated $\mu_0 H_{c2}(0)$ is $\gtrsim 70$ T [86], which makes it comparable with other iron-based and cuprate superconductors [144, 148, 149]. Similar to the iron-pnictide superconductors, the anisotropy for the 11 system is small. For instance, in $\text{Fe}_{1.03}\text{Te}_{0.7}\text{Se}_{0.3}$, the anisotropy coefficient γ (ratio of $\mu_0 H_{c2}$ measured in and out of plane) is less than 2 [32].

A number of groups have reported similar phase diagrams for $\text{Fe}_{1+y}\text{Te}_{1-x}\text{Se}_x$ [53–58]; one version, obtained from magnetization measurements, is shown in figure 9. At first glance, this phase diagram is similar to those of the cuprate [5–9] and iron-pnictide superconductors [38, 40–55, 57, 58]. The undoped compound is an antiferromagnet; with doping, the transition temperature is reduced, and superconductivity appears above 0.1 Se doping (see [53–55]), with T_c vs doping x having a dome shape. However, there are several important differences which need to be pointed out: i) Unlike most other high- T_c superconductors, where “doping” refers to substitution of elements with a different valence, here the replacement of Te with Se is isovalent. The positive hall coefficient in $\text{Fe}_{1.03}\text{Te}_{0.7}\text{Se}_{0.3}$ indicates that hole-carriers are dominant with Se doping [32]; ii) Superconductivity survives to $x = 1$, unlike most other systems where superconductivity disappears with carrier doping above a certain value [90]; iii) The material’s properties can be tuned not only by doping with Se, but also by adjusting the amount of excess Fe. For example, a number of studies of $\text{Fe}_{1+y}\text{Te}_{1-x}\text{Se}_x$ with $x \lesssim 0.5$ have shown that the presence of Fe interstitials correlates with a reduction in superconducting volume fraction [110, 116, 150–152]. Without Se, it appears difficult to reduce Fe content below $y = 0.05$, but the minimum interstitial density decreases as Se is added [140]. The relationship between excess Fe and the magnetic correlations will be discussed in section 4.

3.2. Pressure study on the 11 system

In figure 10 we plot the pressure dependence of T_c for four samples. For Fe_{1+y}Se , there is a strong pressure dependence [153–156]. Applying a pressure of 1.48 GPa raises T_c to 27 K and $\mu_0 H_{c2}(0)$ to 72 T [157]. With further increase of pressure, T_c appears to have a maximum of 37 K for pressures above 4 GPa [153–155]. While T_c increases with pressure, the superconducting volume fraction is reported to decrease rapidly for pressure (P) > 1.5 GPa, suggesting significant inhomogeneity [158]. Margadonna *et al.* [154] also found that the T_c - P curve coincides with anomalies in the pressure evolution of the interlayer spacing, suggesting an intimate relationship between structure and superconductivity.

In the compound with mixed Se and Te, the pressure dependence of T_c is similar to that in Fe_{1+y}Se , though less dramatic [159, 160, 162]. In $\text{FeTe}_{0.5}\text{Se}_{0.5}$, the T_c onset increases rapidly from 13.5 to 26.2 K upon application of a pressure of 2 GPa [159]. Above 2 GPa, T_c decreases linearly, and a metallic (non-superconducting) ground state is observed at 14 GPa [159]. In other Se-doped samples, *e.g.*, $\text{FeTe}_{0.43}\text{Se}_{0.57}$ and $\text{FeTe}_{0.75}\text{Se}_{0.25}$, the pressure effects are reported to be smaller [57, 160, 162].

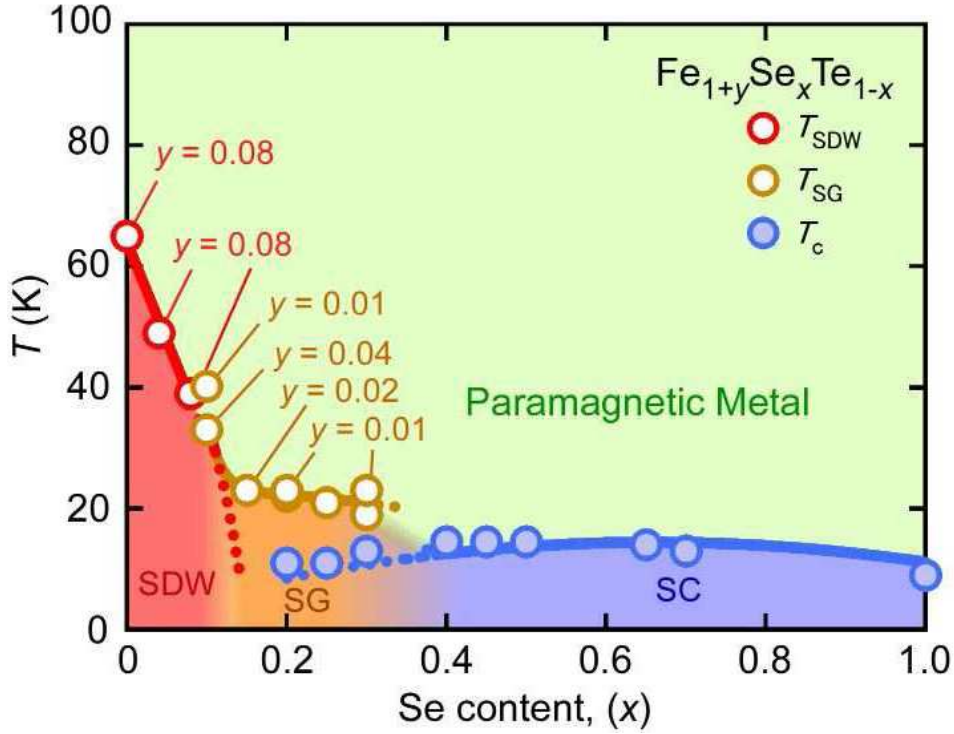


Figure 9. Phase diagram of $\text{Fe}_{1+y}\text{Te}_{1-x}\text{Se}_x$ with $y = 0$ as a function of x and T , constructed from single crystal bulk magnetization data. The nominal Fe content is $y = 0$, unless it is specified. SDW, SG and SC stand for long-range antiferromagnetic, spin-glass and superconducting order respectively. Reprinted from [56]. © 2010 Physical Society of Japan.

For $\text{FeSe}_{0.8}\text{S}_{0.2}$, a study with pressure up to 0.76 GPa shows only a weak effect on T_c , with an indication of a decline in T_c at higher pressure [160]. Contrary to the pressure enhancement of T_c discussed so far, application of pressure to $\text{Fe}_{1+y}\text{Te}_{1-x}\text{S}_x$ causes T_c to decrease monotonically, as shown in figure 10 [161]. One might guess that applying pressure to the parent compound of the 11 system, Fe_{1+y}Te , could make it superconducting; however, superconductivity was not observed in $\text{Fe}_{1.09}\text{Te}$ with hydrostatic pressure up to 2.5 GPa [163], although the structural transition temperature was reduced [163], and the lattice collapsed [164]. In contrast, superconductivity with T_c up to 13 K has indeed been reported for thin film samples of FeTe under tensile stress [165].

3.3. Doping with 3d transition metals into $\text{Fe}_{1+y}\text{Te}_{1-x}\text{Se}_x$

One can also change the properties of the 11 system by doping with 3d transition metals (Mn, Co, Ni, Cu, etc). There are several initial studies on Fe_{1+y}Se [92, 166–168]. Thomas *et al.* [166] have found that 2.5% Co reduces T_c to below 4 K, and no superconductivity is observed for Co doping at and above 5%, though the system is still metallic with 20% Co [143]. Cu seems to have a larger effect in reducing T_c . As little as 1.5% Cu

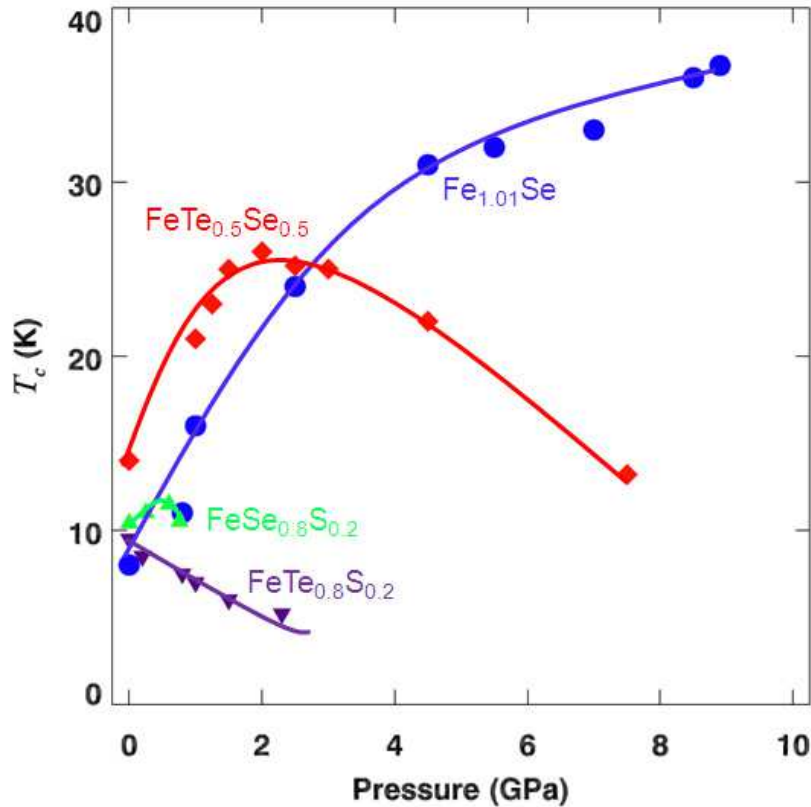


Figure 10. Pressure dependence of the T_c for $\text{Fe}_{1.01}\text{Se}$, [153] $\text{FeTe}_{0.5}\text{Se}_{0.5}$, [159] $\text{FeSe}_{0.8}\text{S}_{0.2}$, [160] and $\text{FeTe}_{0.8}\text{S}_{0.2}$. [161]

substitution results in the absence of a diamagnetic response [167]. More interestingly, with increased Cu doping (4%), the system evolves into an insulator [167, 168]. Analysis of the temperature dependence of the resistivity suggests that the sample with 10% Cu doping is a Mott insulator [168]. This result has interesting implications for the nature of electronic correlations in the iron chalcogenides. Ni doping is also found to suppress T_c [143, 169], but does not drive the system to an insulating state for Ni concentrations up to 20% [143]. Mn substitution has little effect on T_c , and the system remains metallic and superconducting with Mn doping up to 5.5% [168].

Similar studies have been carried out in $\text{Fe}_{1+y}\text{Te}_{1-x}\text{Se}_x$ with $x = 0.35$ [170] and 0.5 [171]. It is found that Co, Ni, and Cu all suppress T_c [170], and a metal-to-insulator transition is induced with both Co and Ni doping in $\text{FeTe}_{0.5}\text{Se}_{0.5}$ samples [171]. There is also a report on Ni-doped $\text{Fe}_{1.1}\text{Te}$, which reveals that the lattice constants decrease with increasing Ni content [172].

3.4. Superconductivity in $A_x\text{Fe}_{2-y}\text{Se}_2$ ($A = \text{K}, \text{Rb}, \text{Cs}, \text{Tl}, \text{Tl/K}, \text{Tl/Rb}$)

At the end of the year 2010, Guo *et al.* [97] reported that superconductivity with T_c above 30 K had been achieved in a ternary iron chalcogenide, $\text{K}_{0.8}\text{Fe}_2\text{Se}_2$ by intercalating the metal K in between FeSe layers. In figure 11 we show results for the

temperature dependence of the magnetization and in-plane resistivity for a $\text{K}_{0.8}\text{Fe}_2\text{Se}_2$ single crystal [128]. The T_c was ~ 32.5 K, the highest among all iron-chalcogenide superconductors at ambient pressure. This new superconductor with such a high T_c soon ignited another wave of intensive activity. To-date, besides $\text{K}_x\text{Fe}_{2-y}\text{Se}_2$ [97, 98, 123, 173–179], superconductivity has been found in a series of compounds with the formula $A_x\text{Fe}_{2-y}\text{Se}_2$ where $A = \text{Rb}, \text{Cs}, \text{Tl}, \text{Tl/K},$ or Tl/Rb [99–101, 124, 125, 180–184, 184, 185], and the highest T_c achieved so far is ~ 33 K. By substituting S ($\text{K}_x\text{Fe}_{2-y}\text{Se}_{2-z}\text{S}_z$), T_c does not decrease for z up to 0.4 [186, 187], but with $z = 1.6$, superconductivity is completely suppressed [186]. In contrast, Co doping in $\text{K}_{0.8}\text{Fe}_2\text{Se}_2$ has a very strong effect. With 0.5% Co, T_c is reduced to 5 K [188]. A number of the newly discovered $A_x\text{Fe}_{2-y}\text{Se}_2$ superconductors and their T_c 's are summarized in table 1, from which one can see that the T_c is not very sensitive to the stoichiometry, except for the Co-doped sample.

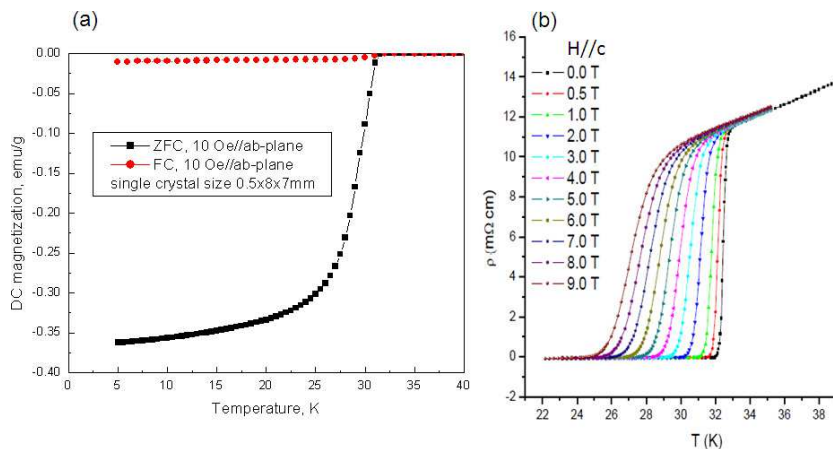


Figure 11. (a) Temperature dependence of the magnetization for a $\text{K}_{0.8}\text{Fe}_2\text{Se}_2$ single crystal. (b) Resistivity measured in the a - b plane with field applied along the c axis [128].

There have been some pressure studies on these systems. In a $\text{K}_x\text{Fe}_2\text{Se}_2$ sample, which had a T_c of 32.6 K, T_c decreased with increasing pressure, while in a sample with a T_c of 31.1 K, a dome-shaped T_c - P curve was observed, with a maximum T_c of 32.7 K at 0.48 GPa [193]. A similar dome shape was observed for $\text{Cs}_x\text{Fe}_2\text{Se}_2$, with T_c maximized to 31.1 K at $P = 0.82$ GPa, compared to 30 K at ambient pressure [193]. In a sample with nominal composition of $\text{K}_{0.8}\text{Fe}_2\text{Se}_2$, which had a T_c of 33 K, it was found that, although the onset T_c increased with pressure, the temperature where the resistivity reached zero decreased [198]. In all of the samples studied, the large normal-state resistance was greatly reduced by pressure [182, 193, 198, 199]. In $\text{Cs}_{0.8}\text{Fe}_2\text{Se}_2$, the resistance decreased by two orders of magnitude, concomitant with a sudden T_c reduction at ~ 8 GPa [182].

In the normal state of these materials, the resistivity-temperature curve exhibits a very pronounced hump [97], which is believed to be irrelevant to superconductivity [122,

Table 1. Summary of T_c for the newly discovered $A_x\text{Fe}_{2-y}\text{Se}_2$ superconductors.

Material	T_c (K)	Material	T_c (K)
$\text{K}_{0.8}\text{Fe}_2\text{Se}_2$ [97, 98, 123, 176, 179, 181]	30-33	$\text{K}_{0.8}\text{Fe}_2\text{Se}_{0.8}\text{S}_{1.2}$ [186]	18.2
$\text{K}_{0.8}\text{Fe}_{1.6}\text{Se}_2$ [189]	32	$\text{K}_{0.8}\text{Fe}_{1.995}\text{Co}_{0.005}\text{Se}_2$ [188]	5
$\text{K}_{0.8}\text{Fe}_{1.76}\text{Se}_2$ [178]	32	$\text{Rb}_{0.83(2)}\text{Fe}_{1.70(1)}\text{Se}_2$ [180]	31.5
$\text{K}_{0.65}\text{Fe}_{1.41}\text{Se}_2$ [190]	32	$\text{Rb}_{0.8}\text{Fe}_2\text{Se}_2$ [181, 191]	32
$\text{K}_{0.85}\text{Fe}_{1.83}\text{Se}_{2.09}$ [192]	30	$\text{Rb}_{0.88}\text{Fe}_{1.81}\text{Se}_2$ [99]	31.5
$\text{K}_{0.85}\text{Fe}_2\text{Se}_{1.8}$ [193]	32.6	$\text{Cs}_{0.86}\text{Fe}_{1.66}\text{Se}_2$ [124, 181, 193]	30
$\text{K}_{0.86}\text{Fe}_2\text{Se}_{1.82}$ [124, 193]	31.1	$\text{Cs}_{0.83(2)}\text{Fe}_{1.71(1)}\text{Se}_{1.96}$ [183]	28.5
$\text{K}_{0.7}\text{Fe}_{1.8}\text{Se}_2$ [177]	28	$\text{Cs}_{0.8}\text{Fe}_2\text{Se}_2$ [182]	32
$\text{K}_{0.86}\text{Fe}_{1.73}\text{Se}_2$ [175]	25	$\text{TlFe}_{1.7}\text{Se}_2$ [125]	22.8
$\text{K}_{0.86}\text{Fe}_{1.84}\text{Se}_2$ [174]	30	$\text{Tl}_{0.58}\text{K}_{0.42}\text{Fe}_{1.72}\text{Se}_2$ [101, 194]	32
$\text{K}_{0.83(1)}\text{Fe}_{1.66(1)}\text{Se}_2$ [180]	29.5	$\text{Tl}_{0.64}\text{K}_{0.36}\text{Fe}_{1.83}\text{Se}_2$ [125]	31
$\text{K}_{0.8}\text{Fe}_{1.7}\text{SeS}$ [195]	25	$\text{Tl}_{0.63}\text{K}_{0.37}\text{Fe}_{1.78}\text{Se}_2$ [196]	29
$\text{K}_{0.8}\text{Fe}_2\text{Se}_{1.4}\text{S}_{0.4}$ [187]	32.8	$\text{Tl}_{0.47}\text{Rb}_{0.34}\text{Fe}_{1.63}\text{Se}_2$ [197]	33
$\text{K}_{0.8}\text{Fe}_2\text{Se}_{1.6}\text{S}_{0.4}$ [186]	33.2	$\text{Tl}_{0.58}\text{Rb}_{0.42}\text{Fe}_{1.72}\text{Se}_2$ [101]	32
$\text{K}_{0.8}\text{Fe}_2\text{Se}_{1.2}\text{S}_{0.8}$ [186]	24.6	$\text{Tl}_{0.4}\text{Rb}_{0.4}\text{Fe}_{2-y}\text{Se}_2$ [184]	31.8

181, 193]. However, in $\text{K}_{0.8}\text{Fe}_{1.7}\text{Se}_2$, Guo *et al.* [199] found an interesting correlation between superconductivity and the hump: with increasing pressure, the magnitude of the hump went down as T_c did, and the hump disappeared at $P = 9.2$ GPa, in coincidence with the complete suppression of the superconductivity. By normalizing the resistance to the room-temperature value, Seyfarth *et al.* [182] found that the hump still existed at $P = 9$ GPa, at which pressure the sample was not superconducting; based on this, they concluded that the hump was not related to the superconductivity.

These newly discovered superconductors are particularly interesting and fundamentally important in part due to their electronic structures. First-principle calculations have shown that the band structure in this new system is quite different from that of other iron-based superconductors [200–205]. In particular, the band near the Brillouin zone center Γ point sinks well below the Fermi level [200–205]. Experimentally, this prediction has been verified by several initial angle-resolved photoemission spectroscopy (ARPES) studies, which show that there is no hole pocket near the Γ point [206, 207]. Instead, there are electron pockets near both the Γ and M (Brillouin zone corner) points [194, 196, 208]. Although this result does not rule out the possibility that inter-band scattering between the electron pockets at Γ and M could be important to the superconductivity [209], the sign-changed s_{\pm} pairing symmetry which has been suggested in other iron-based superconductors is not likely to apply here [62, 63, 210]. Several alternatives, including d -wave [209, 211], s -wave [212, 213], and s_{++} -wave [214] superconductivity have been proposed theoretically. A number of ARPES [194, 196, 206–208], nuclear magnetic resonance (NMR) [176, 179, 215], and specific heat measurements [173]

have been carried out and all of them indicate that the gap is nodeless.

Another interesting feature which distinguishes the $A_x\text{Fe}_{2-y}\text{Se}_2$ superconductors from other iron-based superconductors is that their superconductivity is in close vicinity to an insulating state, similar to the case of cuprate superconductors [5–9], but not to that of other iron-based superconductors [94]. Interestingly, it is reported that the insulating $\text{K}_x\text{Fe}_{2-y}\text{Se}$ sample becomes superconducting by annealing and quenching, and after a few days at room temperature, it is insulating again, showing that the insulating and superconducting states are reversible [216]. Based on these observations, it is suggested that disordering of Fe vacancies plays a key role in rendering the superconductivity [216]. The experimentally observed insulating ground state [125, 181, 186, 195, 217] has stimulated several theoretical calculations [200, 201, 218]. Two possible origins of the insulating behaviour have been proposed which are to be verified experimentally: the system might be a Mott insulator [195, 205, 218, 219] (the Mott behaviour may have a complex origin where both Fe vacancies and $3d$ electron-electron correlations play roles as suggested in [205]), or it might be a band insulator resulting from the electronic structure reconstruction due to ordered Fe vacancies [200, 201].

3.5. Summary

To summarize this section, it is found that the parent compound for the 11 system, Fe_{1+y}Te , is non-superconducting, and superconductivity is achieved by replacing Te with Se or S. The optimal superconductivity with T_c of 14 K is found to be in samples with $y = 0$ and $x \approx 0.5$. Fe_{1+y}Se is where superconductivity was initially discovered for the 11 system; it has a T_c of 8 K. The T_c increases to ~ 37 K upon application of hydrostatic pressure. The superconductivity seems to be vulnerable to doping with $3d$ transition metals, which can tune the system to a (possibly Mott) insulating regime. More recently, a series of ternary iron-chalcogenide compounds with the chemical formula $A_x\text{Fe}_{2-y}\text{Se}$ were found to be superconducting with T_c up to 33 K, the highest among all Fe-Se-based superconductors at ambient pressure.

4. Magnetic correlations

4.1. Magnetic order

4.1.1. $\text{Fe}_{1+y}\text{Te}_{1-x}\text{Se}_x$ system The magnetic order in $\text{Fe}_{1+y}\text{Te}_{1-x}\text{Se}_x$ has attracted considerable attention because of its rich physics. An initial band-structure calculation predicted that the Fermi-surface topology in this system should be similar to that of the iron pnictides [220]; this has been confirmed by ARPES measurements [221, 222]. From the Fermi-surface-nesting picture [220], one would expect that this system would have collinear (C-type) spin-density-wave (SDW) order with an in-plane wave vector $(0.5, 0.5)$, assuming a unit cell containing two irons as shown in figure 12(b). However, several decades ago, Fruchart *et al.* [223] determined that the magnetic ordering vector is $(0.5, 0)$ in $\text{Fe}_{1.125}\text{Te}$. This result has been confirmed by Bao *et al.* [138] in $\text{Fe}_{1.075}\text{Te}$, and

by Li *et al.* [139] in $\text{Fe}_{1.068}\text{Te}$; each of these has a bicollinear (E-type) spin structure as shown in figure 12(a). Even more surprising is the fact that ARPES measurements have observed no SDW nesting instability along $(0.5, 0)$, although there is a weak hole pocket around the X point [221, 224]. Clearly, a simple nesting mechanism cannot account for these experimental results. More recent first-principle calculations have identified the role of local-moments and the importance of Hund’s exchange coupling, and have provided better agreement with the experimental observations [43, 75, 225–229].

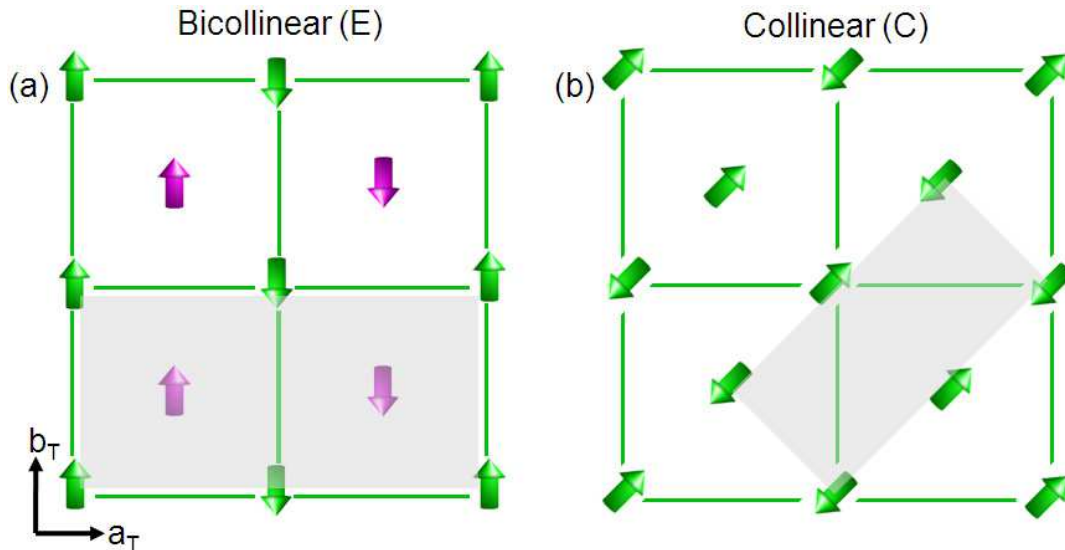


Figure 12. (a) Schematic for the bicollinear (E-type) in-plane spin structure in tetragonal notation of the 11 compound. (b) Collinear (C-type) magnetic structure for iron pnictides. Shadow represents the magnetic unit cell.

The magnetic order in Fe_{1+y}Te is long-ranged, with a maximum moment size of $\sim 2.5 \mu_B/\text{Fe}$ for $y = 0.05$ [140]; the moment size decreases for larger y [138, 139, 223]. The moment size is significant compared to that in iron-pnictide antiferromagnets, but it is small compared to the effective moment estimated from the magnetic susceptibility in the paramagnetic phase [230]. The moment is found to be aligned mostly along the b axis as shown in figure 12(a) [138–140]. Bao *et al.* [138] have shown that the order can be commensurate or incommensurate depending upon the amount of excess Fe—with more Fe, the incommensurability is larger. Upon doping with Se, the order is suppressed, with a reduced ordering temperature (from 65 to $\lesssim 30$ K with 0.1 Se) [56], reduced size of the ordered magnetic moment (from 2.1 to $0.27 \mu_B/\text{Fe}$) [54], and shorter correlation length (the magnetic peak is resolution limited in the parent compound, while with 0.25 Se doping, the order is short-ranged with a correlation length of $\sim 4 \text{ \AA}$ [113, 138]). For Se content above 0.15, there is a phase where spin-glass order and superconductivity coexist [53, 54, 56, 113, 140]. In two single crystal samples, $\text{Fe}_{1.07}\text{Te}_{0.75}\text{Se}_{0.25}$ and $\text{FeTe}_{0.7}\text{Se}_{0.3}$, both exhibiting short-range incommensurate order below 40 K, it is found that with increasing excess Fe, the incommensurability is larger, similar to the case in the parent compound [113, 138]. In $\text{FeTe}_{0.7}\text{Se}_{0.3}$, which has more Se and less Fe than the

Fe_{1.07}Te_{0.75}Se_{0.25} sample, the spin-glass order is depressed, with weaker peak intensity and shorter correlation length, while superconductivity is enhanced, with higher T_c and superconducting volume fraction [113]. Interestingly, a magnetic peak is only observed on one side of the commensurate wave vector $(0.5, 0)$, [*i. e.* $(0.5-\delta, 0)$ and not $(0.5\pm\delta, 0)$ with δ being the incommensurability]; this is likely a result of an imbalance of ferromagnetic/antiferromagnetic correlations between neighbouring spins [113]. (A closely related picture of spin clusters is indicated by a recent study of Fe_{1.1}Te [230].) With further increase of the Se concentration, the superconductivity optimizes with $x \approx 0.5$, and no static magnetic order is observed (for $y \sim 0$) [53, 54, 86].

Next, we turn to the intriguing case of superconducting Fe_{1+y}Se. Although this system exhibits a symmetry-lowering structural transition on cooling through ~ 90 K [134, 135, 137], measurements with local probes such as Mössbauer spectroscopy [103, 137] and ⁷⁷Se NMR [231] indicate an absence of static magnetic order. This is in sharp contrast with the case of Fe_{1+y}Te; nevertheless, NMR measurements indicate that spin fluctuations increase on cooling towards T_c [231]. In studies of a sample that showed an increase of T_c to 37 K under pressure, Mössbauer measurements indicated an absence of magnetic order up to ~ 30 GPa [153]. NMR measurements on the same material found that spin fluctuations are enhanced under pressure, along with the superconductivity [231]. In contrast, Bendele *et al.* [232] reported evidence for short-range magnetic order for $P \gtrsim 0.8$ GPa based on muon-spin rotation (μ SR) measurements; however, this sample showed a much more modest impact of pressure on the superconductivity, with a maximum T_c of 13 K at 0.7 GPa. Mössbauer studies have shown that doping Cu into Fe_{1+y}Se induces a local magnetic moment, with the size of the moment increasing with Cu doping while superconductivity is suppressed [167]. Spin-glass behavior has been inferred from magnetization measurements on these Cu-doped samples [167].

The magnetic and superconducting phases in Fe_{1+y}Te_{1-x}Se_x are summarized in figure 9. Overall, the behaviour is consistent with the common belief that static magnetic order competes with superconductivity, while spin fluctuations promote it.

4.1.2. A_xFe_{2-y}Se₂ materials Antiferromagnetic order was found in TlFe_{2-y}Se₂ by neutron and Mössbauer measurements [233, 234] long before the recent discovery of superconductivity in the related A_xFe_{2-y}Se₂ compounds. Bao *et al.* [189] have recently used neutron powder diffraction to determine the crystalline and magnetic structure for K_xFe_{2-x}Se₂. At high temperature, the crystal structure is equivalent to that of the 122 materials. At lower temperature, the Fe vacancy order drives the system to an $I4/m$ phase with an enlarged unit cell of $\sqrt{5} \times \sqrt{5} \times 1$ [235], which contains a pair of the Fe-Se layers related by inversion symmetry [189]. It is found that T_N is as high as 559 K and that the magnetic moment is as large as 3.31 μ_B /Fe, forming a collinear antiferromagnetic structure with (101) being the propagation wave vector [217]. The moment points mainly along the c axis [189]. Such a collinear magnetic structure has been reproduced by several theoretical works [200, 201, 219, 236]. It is intriguing

that the magnetic order occurs in a tetragonal phase without breaking the four-fold symmetry, although the presence of Fe vacancies may reduce any magnetic frustration [219]. More surprisingly, it has been reported that superconductivity coexists with the strong antiferromagnetic order, both in the neutron study of $\text{K}_{0.8}\text{Fe}_2\text{Se}_2$ [189] and in the μSR study of $\text{Cs}_{0.8}\text{Fe}_2\text{Se}_{1.96}$ [185]. There have been many further observations of the coexistence of superconductivity and antiferromagnetic order [180, 183, 184, 192, 237]. However, due to the difficulty in obtaining samples with high superconducting volume fractions, as well as evidence pointing to phase separations [132, 133, 181, 216, 238–240], it is not yet clear whether the superconductivity and antiferromagnetic order coexist locally or in different regions of a sample.

4.2. Spin excitations in $\text{Fe}_{1+y}\text{Te}_{1-x}\text{Se}_x$

4.2.1. *Spin dynamics near (0.5, 0.5)* The “resonance” mode in the magnetic excitations, which is defined as the energy at which there is a significant increase in spectral weight when the system enters the superconducting phase, has been the subject of extensive measurements. The resonance is predicted to occur at a particular wave vector if it connects portions of the Fermi surface that have opposite signs of the superconducting gap function. Therefore, observations of the resonance may provide important information relevant to the pairing symmetry [241–244]. (Note that these analyses make the assumption that the magnetism is due to the same electrons that participate in the superconductivity, while the validation of the assumption is still under debate. [115, 224, 245]) Resonance excitations have been observed in a number of iron-based superconductors [78, 83], consistent with the presumed gap-sign change between the hole and electron pockets [210]. In $\text{Fe}_{1+y}\text{Te}_{1-x}\text{Se}_x$, despite the fact that the magnetic ordering wave vector is different from that of iron pnictides by 45° , the resonance excitation was observed to be near the same (0.5, 0.5) wave vector by several groups [84–86, 115, 246–248]. Compared to the magnetic excitation spectrum above T_c , the low-temperature spectral weight is greatly enhanced around (0.5, 0.5) and the resonance energy of ~ 6.5 meV, as shown in figure 13(c) [84]. The resonance energy corresponds to $\sim 5k_B T_c$, similar to the situation in other high- T_c superconductors [90]. Accompanying the resonance, there is a spin gap with an energy of ~ 4 meV; the intensity below the spin gap is shifted to the resonance in the superconducting state [84, 86].

Interestingly, it is found that the resonance is incommensurate in \mathbf{Q} , peaking at $(0.5 \pm \delta, 0.5 \mp \delta)$, in a direction transverse to (0.5, 0.5) [115]. Results on the \mathbf{Q} dependence of the magnetic response at 6.5 meV are plotted in figure 14. Transverse scans along $[1\bar{1}0]$ exhibit a pair of peaks as shown in figure 14(a), while longitudinal scans show a single broad peak centered at (0.5, 0.5), as shown in figure 14(b). In both cases, the intensity is enhanced when the sample is cooled below T_c . The color-coded plot of intensity *vs* \mathbf{Q} at 6.5 meV and $T = 1.5$ K, figure 14(c), demonstrates an intriguing anisotropy: the transverse peaks are not reproduced along the longitudinal direction.

For other energies, the anisotropy still persists [85, 246–249], showing that the

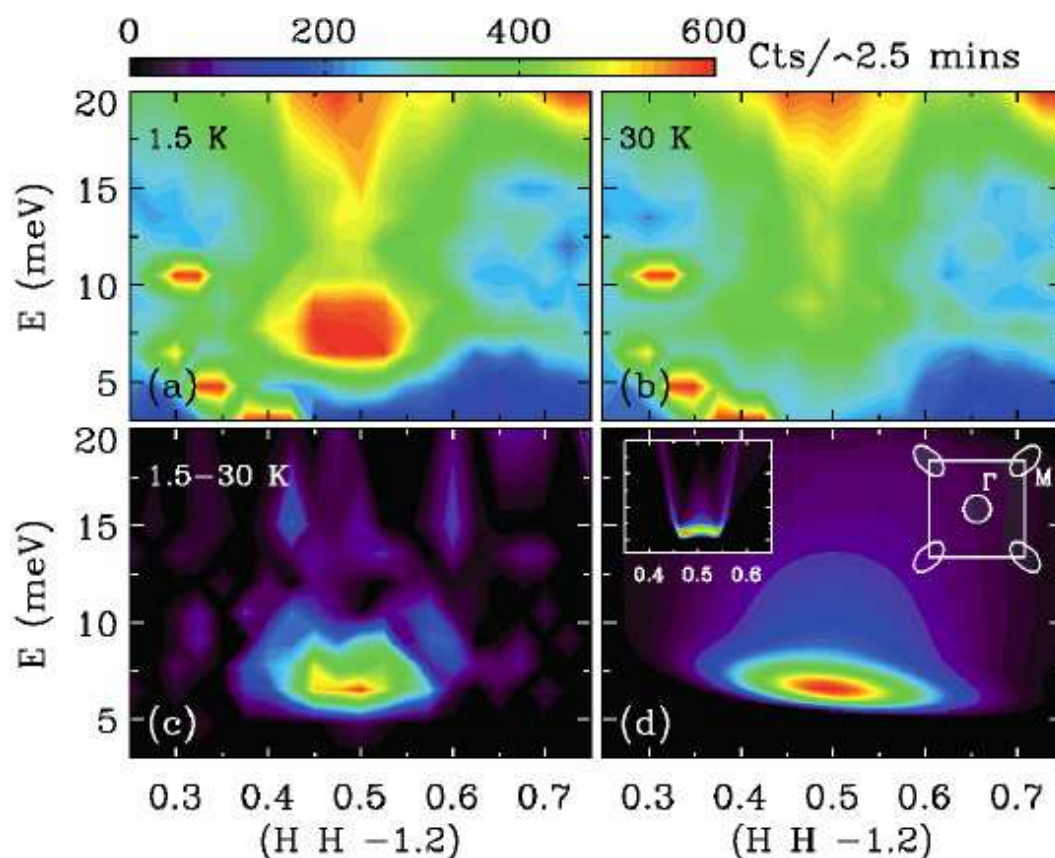


Figure 13. Spin resonance in $\text{FeTe}_{0.6}\text{Se}_{0.4}$. (a) and (b) shows the spin excitation spectrum as a function of \mathbf{Q} and energy at 1.5 and 30 K respectively. (c) shows the resonance intensity as determined by the difference between the 1.5 and 30 K spectra. (d) Calculated intensity difference from a simplified two-band model with resolution convolved. The left inset shows the resolution-free calculated intensity and the right inset is the normal-state Fermi surface employed in the calculation. Reprinted from [84]. © 2009 American Physical Society.

magnetic excitations are anisotropic, dispersing only along the direction transverse to $(0.5, 0.5)$, as shown in figure 14(d). This is certainly not a spin-wave like excitation, as in CaFe_2As_2 [250, 251], since in that case one would expect to see a cone-shaped dispersion. ARPES measurements on the sample found that the Fermi surface near $(0.5, 0.5)$ appears to consist of four incommensurate pockets [115]. While Fermi-surface nesting is in principle compatible with the observation of the incommensurate resonance, the dispersion of isolated intensity peaks along a single direction is quite unusual and requires consideration of coupling of spin and orbital effects [115].

Since superconductivity, and hence the pairing, is sensitive to magnetic field, one would naturally expect that an external magnetic field could impact the resonance, as seen in $\text{YBa}_2\text{Cu}_3\text{O}_{6.6}$ [252] and in $\text{La}_{1.82}\text{Sr}_{0.18}\text{CuO}_4$ [253]. Qiu *et al.* [84] found no significant change in the resonance in $\text{FeTe}_{0.6}\text{Se}_{0.4}$ in the presence of a 7-T field on a cold-neutron spectrometer with low flux. Another experiment on $\text{FeTe}_{0.5}\text{Se}_{0.5}$ using

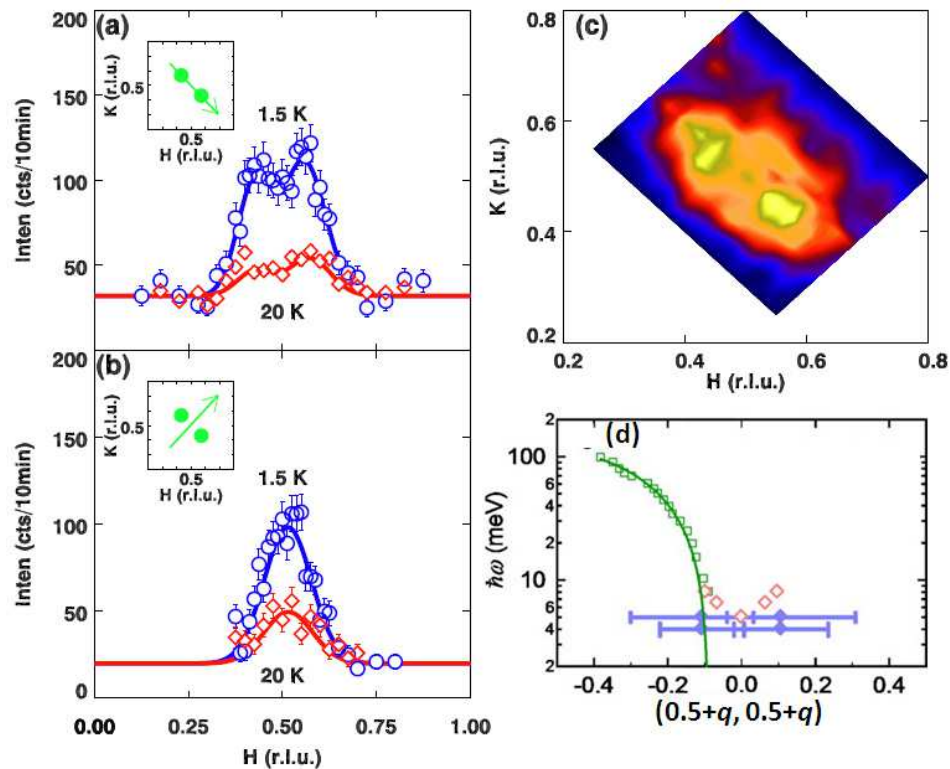


Figure 14. Incommensurate resonance in \mathbf{Q} , peaking at $(0.5 \pm \delta, 0.5 \mp \delta)$, transversely to $(0.5, 0.5)$, at $\hbar\omega = 6.5$ meV. (a) and (b) show the \mathbf{Q} scans at 1.5 and 20 K, below and above T_c , with scan directions shown in the left insets. Upper right inset is obtained by subtracting 20-K data from 1.5-K data. (c) is the plot of the \mathbf{Q} dependence of the intensity at 6.5 meV at 1.5 K. (d) shows the dispersion from $(0.5, 0.5)$ in semi-log scale. (a)-(c) reprinted from [127]. (d) reprinted from [115]; © 2010 American Physical Society.

a spectrometer with higher flux concluded that the resonance starts to appear at a lowered T_c , 12 K, with reduced intensity, due to the suppression of the superconductivity; however, there was no detectable change in either the resonance energy or the width of the resonance peak [86]. With a field of 14.5 T, Zhao *et al.* [254] have shown that in $\text{BaFe}_{1.9}\text{Ni}_{0.1}\text{As}_2$, both the resonance energy and intensity are reduced, and the resonance peak is slightly broadened.

One commonly adopted view is that the spin resonance is a singlet-to-triplet excitation [243, 244, 255]. In principle, this hypothesis can be tested by experiments in magnetic field which should induce a Zeeman splitting and lift the degeneracy of the triplet excited state [252]. Bao *et al.* [256] tried to address this problem by applying a 14-T field on $\text{FeSe}_{0.4}\text{Te}_{0.6}$, and it appears that the field induces a peak splitting. However, a more recent experiment shows that the field only reduces the spectral weight around the resonance mode [257]. We applied a 16-T magnetic field and examined the field effect on the resonance. No splitting was observed in this measurement either. The nature of the resonance mode is still an open question.

4.2.2. *Doping dependence* As discussed above, the non-superconducting parent compound of the 11 system, Fe_{1+y}Te , has static magnetic order with a bicollinear spin configuration. In samples with robust superconducting properties, there is strong magnetic scattering around $(0.5, 0.5)$ with a spin resonance below T_c , corresponding to spin correlations of the collinear type. A number of theoretical [75, 228] and experimental [54, 116, 248, 249] studies have been carried out on the doping evolution of the magnetic correlations (static and dynamic), and their correlation with superconductivity. Lumsden *et al.* [249] have performed measurements on time-of-flight spectrometers which cover a large momentum-energy space on two samples, a non-superconducting $\text{Fe}_{1.04}\text{Te}_{0.73}\text{Se}_{0.27}$, and a superconducting $\text{FeTe}_{0.51}\text{Se}_{0.49}$. It is clearly shown in figure 15(a) that at 5-7 meV, for the non-superconducting sample, the spectral weight is mostly concentrated around $(0.5, 0)$, where static magnetic order is observed. For the superconducting sample, magnetic excitations with a spin resonance near $(0.5, 0.5)$ are dominant, as shown in figure 15(b). On the other hand, the high-energy (> 120 meV) spectrum looks qualitatively similar for these two samples [249]. In the non-superconducting parent compound, $\text{Fe}_{1.05}\text{Te}$, spin waves dispersing up to ~ 250 meV have been measured by Lipscombe *et al.* [258]. These have been modelled in terms of spin waves calculated from a Heisenberg Hamiltonian with nearest- and next-nearest-neighbour couplings [258]; however, a recent study of $\text{Fe}_{1.1}\text{Te}$, identifying distinct patterns of diffuse scattering and anomalous thermal enhancement of the effective moment, raises questions about such an approach [230].

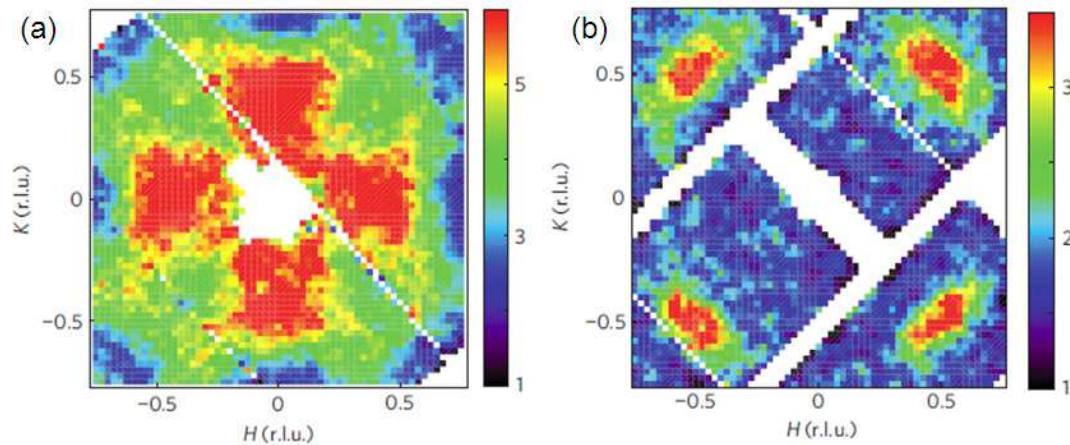


Figure 15. (a) Constant-energy cut of the magnetic excitation spectrum at an energy transfer of 6 ± 1 meV for the non-superconducting sample $\text{Fe}_{1.04}\text{Te}_{0.73}\text{Se}_{0.27}$ at 5 K. (b) Plot for the superconducting sample $\text{FeTe}_{0.51}\text{Se}_{0.49}$ at 3.5 K. Reprinted from [249]. © 2010 Macmillan Publishers Ltd.

As mentioned previously, the properties of $\text{Fe}_{1+y}\text{Te}_{1-x}\text{Se}_x$ are sensitive not only to the Se concentration, but also to the amount of excess Fe. Xu *et al.* [116] demonstrated this by measuring the magnetic spectrum around $(0.5, 0)$ and $(0.5, 0.5)$ in four samples: $\text{FeTe}_{0.7}\text{Se}_{0.3}$, $\text{Fe}_{1.05}\text{Te}_{0.7}\text{Se}_{0.3}$; $\text{FeTe}_{0.5}\text{Se}_{0.5}$, and $\text{Fe}_{1.05}\text{Te}_{0.55}\text{Se}_{0.45}$. Both samples with

$y = 0$ are superconducting with the same T_c of 14 K; a resonance in the spin excitation spectrum is observed below T_c near $(0.5, 0.5)$, although the one with $x = 0.3$ has a smaller superconducting volume fraction, and less spectral weight around $(0.5, 0.5)$. Also, there is short-range static magnetic order near $(0.5, 0)$ in $\text{FeTe}_{0.7}\text{Se}_{0.3}$, while the sample with $x = 0.5$ does not exhibit magnetic order, short- or long-ranged, and the low-energy excitations close to $(0.5, 0)$ also disappear. With 0.05 extra Fe, superconductivity in both samples is fully suppressed, leading to the absence of the resonance, and the spectral-weight transfers from $(0.5, 0.5)$ to $(0.5, 0)$. In both samples, there is short-range static order and strong spectral weight around $(0.5, 0)$. Recently, Stock *et al.* [259] have shown that by changing y in Fe_{1+y}Te , the low-energy magnetic excitation spectrum can be dramatically modified, thus demonstrating the important role of excess Fe.

4.3. Summary

In the parent compound of the 11 system, there is long-range antiferromagnetic order with an ordering temperature of 65 K, and an in-plane wave vector $(0.5, 0)$; importantly, no Fermi-surface nesting is found along this wave vector. The direction of the wave vector is different from that of the iron pnictides by 45° . The magnetic ordering wave vector can become incommensurate with larger amounts of excess Fe.

Upon Se doping, the antiferromagnetic order is suppressed and becomes short-ranged, followed by the appearance of superconductivity. For samples with $x \approx 0.5$ and robust superconductivity, there is no static order, and the low-energy spin excitations around $(0.5, 0)$ also disappear. The spectral weight is shifted to $(0.5, 0.5)$, where an incommensurate spin resonance is observed; the spin resonance is demonstrated to be intimately tied to the superconductivity from both the temperature and magnetic-field dependence. The magnetic excitation spectrum around $(0.5, 0.5)$ shows an interesting anisotropy, which apparently cannot be explained by either a Fermi-surface-nesting or a local-moment model. In Fe_{1+y}Se , there is no static order, while there are spin fluctuations which are enhanced near T_c . The superconducting and magnetic properties of the system can also be modified by adjusting the amount of excess Fe with fixed Se content. The extra Fe is found to enhance the magnetic correlations around $(0.5, 0)$ and suppress superconductivity as well as the spin excitations around $(0.5, 0.5)$.

The results on the evolution of the magnetic excitation spectrum with the tuning parameters (Se/Fe), clearly indicate that static bicollinear magnetic order in the 11 system competes with superconductivity. It appears that only when the system evolves towards fluctuating collinear magnetic correlations, does superconductivity appear; this seems to be universal across all known iron-based superconductor families. Despite these agreements, the origin of the magnetism in the 11 compound is quite controversial. Some believe that the magnetism arises from itinerant electrons [85, 246]. Recently there has been work suggesting a large local moment associated with the low-energy magnetic excitations in a superconducting $\text{FeTe}_{0.35}\text{Se}_{0.65}$ sample; this observation is incompatible with predictions from a weakly coupled itinerant picture [260]. The

fact that a simple Fermi-surface-nesting picture [220] cannot explain many of the experimental observations [115, 138, 221, 260] leads to arguments for a significant local-moment character to the magnetism [43, 221, 224–229].

For the $A_x\text{Fe}_{2-y}\text{Se}_2$ system, it is found that superconductivity is in close proximity to an insulating phase. This feature is different from that in other iron-based superconductors, but mirrors that in the high- T_c cuprates. Whether the microscopic coexistence of strong antiferromagnetic order with high- T_c superconductivity is true or not requires further investigation. If they do coexist, it requires further studies to understand whether or not the superconducting pairing mechanism in this system is the same as that in other high- T_c superconductors.

5. Conclusions

Thanks to the sustained efforts on sample synthesis for the $\text{Fe}_{1+y}\text{Te}_{1-x}\text{Se}_x$ system, some high-quality samples have been made available. In particular, by using the Bridgman technique, many large-size, high-quality single crystals have been grown. Measurements performed on these samples yield a plethora of fascinating results. It has been found that the static antiferromagnetic order in the parent compound is centered around the wave vector $(0.5, 0)$ with a bicollinear spin structure that competes with superconductivity, while superconducting samples are characterized by collinear magnetic correlations with magnetic excitations centered around the wave vector $(0.5, 0.5)$. The argument that there is an intimate relationship between the spin excitations around $(0.5, 0.5)$ and superconductivity has been reinforced by the temperature and magnetic-field dependence of the resonance. Generally, this system shows strong similarities to other high- T_c superconductors, where it is believed that spin excitations play a progenitive role in the superconductivity.

For the newly discovered $A_x\text{Fe}_{2-y}\text{Se}_2$ superconductors, which have superconducting transition temperatures, T_c , up to 33 K, crystals can be obtained using the Bridgman technique. This system is unique: i) It has a very different Fermi-surface topology with two electron pockets at the Brillouin zone center; ii) The superconducting phase borders an insulating parent phase, as in the case of the cuprates, but different from all previously investigated iron-based superconductors.

While $A_x\text{Fe}_{2-y}\text{Se}_2$ has attracted significant attention, there are still many basic questions to be answered. For instance, reports on the spin dynamics in this system have been very limited [261]. This will provide important clues on whether or not this system shares the same basic physics underlying the superconductivity as other high-temperature superconductors. Also, further efforts on obtaining single crystals with improved sample quality and larger size will certainly be needed in order to elucidate many unresolved issues. For the 11 system, sample inhomogeneity is a less significant issue. Future work to control the stoichiometry more precisely will be helpful.

6. Acknowledgements

The work at Brookhaven National Laboratory (J.W., G.X., G.G., and J.M.T.) was supported by the Office of Basic Energy Sciences, Division of Materials Science and Engineering, U.S. Department of Energy, under Contract No. DE-AC02-98CH10886. J.M.T. is also supported in part by the Center for Emergent Superconductivity, an Energy Frontier Research Center. Work at Lawrence Berkeley National Laboratory (J.W. and R.J.B.) was supported by the same Office under Contract No. DE-AC02-05CH11231. The authors thank all of their collaborators listed in the references. We are also grateful to our colleagues and collaborators for allowing us to reproduce their work here.

References

- [1] H. K. Onnes. The resistance of pure mercury at helium temperatures. *Comm. Leiden.*, 120b, 1911.
- [2] J. Bardeen, L. N. Cooper, and J. R. Schrieffer. Theory of Superconductivity. *Phys. Rev.*, 108:1175, 1957.
- [3] J. G. Bednorz and K. A. Müller. Possible High T_c Superconductivity in the Ba-La-Cu-O system. *Z. Phys. B*, 64:189, 1986.
- [4] M. K. Wu, J. R. Ashburn, C. J. Torng, P. H. Hor, R. L. Meng, L. Gao, Z. J. Huang, Y. Q. Wang, and C. W. Chu. Superconductivity at 93 K in a new mixed-phase Y-Ba-Cu-O compound system at ambient pressure. *Phys. Rev. Lett.*, 58:908, 1987.
- [5] Patrick A. Lee, Naoto Nagaosa, and Xiao-Gang Wen. Doping a Mott insulator: Physics of high-temperature superconductivity. *Rev. Mod. Phys.*, 78:17, 2006.
- [6] E. W. Carlson, V. J. Emery, S. A. Kivelson, and D. Orgad. *The Physics of Conventional and Unconventional Superconductors*, chapter Concepts in High Temperature Superconductivity. Springer-Verlag, 2002.
- [7] R. J. Birgeneau, C. Stock, J. M. Tranquada, and K. Yamada. Magnetic neutron scattering in hole doped cuprate superconductors. *J. Phys. Soc. Jpn.*, 75:111003, 2006.
- [8] M. A. Kastner, R. J. Birgeneau, G. Shirane, and Y. Endoh. Magnetic, transport, and optical properties of monolayer copper oxides. *Rev. Mod. Phys.*, 70:897, 1998.
- [9] J. Orenstein and A. J. Millis. Advances in the Physics of High-Temperature Superconductivity. *Science*, 288:468, 2000.
- [10] Yoichi Kamihara, Hidenori Hiramatsu, Masahiro Hirano, Ryuto Kawamura, Hiroshi Yanagi, Toshio Kamiya, and Hideo Hosono. Iron-Based Layered Superconductor: LaOFeP. *J. Am. Chem. Soc.*, 128:10012, 2006.
- [11] Yoichi Kamihara, Takumi Watanabe, Masahiro Hirano, and Hideo Hosono. Iron-Based Layered Superconductor La[O_{1-x}F_x]FeAs (x=0.05-0.12) with $T_c=26$ K. *J. Am. Chem. Soc.*, 130:3296, 2008.

- [12] X. H. Chen, T. Wu, G. Wu, R. H. Liu, H. Chen, and D. F. Fang. Superconductivity at 43 K in Samarium-arsenide Oxides $\text{SmFeAsO}_{1-x}\text{F}_x$. *Nature*, 453:761, 2008.
- [13] Hiroki Takahashi, Kazumi Igawa, Kazunobu Arii, Yoichi Kamihara, Masahiro Hirano, and Hideo Hosono. Superconductivity at 43 K in an iron-based layered compound $\text{LaO}_{1-x}\text{F}_x\text{FeAs}$. *Nature*, 453:376, 2008.
- [14] Hijiri Kito, Hiroshi Eisaki, and Akira Iyo. Superconductivity at 54 K in F-Free NdFeAsO_{1-y} . *J. Phys. Soc. Jpn.*, 77:063707, 2008.
- [15] Zhi-An Ren, Jie Yang, Wei Lu, Wei Yi, Xiao-Li Shen, Zheng-Cai Li, Guang-Can Che, Xiao-Li Dong, Li-Ling Sun, Fang Zhou, and Zhong-Xian Zhao. Superconductivity in the iron-based F-doped layered quaternary compound $\text{NdO}_{1-x}\text{F}_x\text{FeAs}$. *Euro. Phys. Lett.*, 82:57002, 2008.
- [16] Zhi-An Ren, Wei Lu, Jie Yang, Wei Yi, Xiao-Li Shen, Zheng-Cai Li, Guang-Can Che, Xiao-Li Dong, Li-Ling Sun, Fang Zhou, and Zhong-Xian Zhao. Superconductivity at 55 K in iron-based F-doped layered quaternary compound $\text{SmO}_{1-x}\text{F}_x\text{FeAs}$. *Chin. Phys. Lett.*, 25:2215, 2008.
- [17] Cao Wang, Linjun Li, Shun Chi, Zengwei Zhu, Zhi Ren, Yuke Li, Yuetao Wang, Xiao Lin, Yongkang Luo, Shuai Jiang, Xiangfan Xu, Guanghan Cao, and Zhu'an Xu. Thorium-doping-induced superconductivity up to 56 K in $\text{Gd}_{1-x}\text{Th}_x\text{FeAsO}$. *Euro. Phys. Lett.*, 83:67006, 2008.
- [18] Athena S. Sefat, Rongying Jin, Michael A. McGuire, Brian C. Sales, David J. Singh, and David Mandrus. Superconductivity at 22 K in Co-Doped BaFe_2As_2 Crystals. *Phys. Rev. Lett.*, 101:117004, 2008.
- [19] Marianne Rotter, Marcus Tegel, and Dirk Johrendt. Superconductivity at 38 K in the iron arsenide $\text{Ba}_{1-x}\text{K}_x\text{Fe}_2\text{As}_2$. *Phys. Rev. Lett.*, 101:107006, 2008.
- [20] G. F. Chen, Z. Li, G. Li, W. Z. Hu, J. Dong, X. D. Zhang, P. Zheng, N. L. Wang, and J. L. Luo. Superconductivity in hole-doped $(\text{Sr}_{1-x}\text{K}_x)\text{Fe}_2\text{As}_2$. *Chin. Phys. Lett.*, 25:3403, 2008.
- [21] D. S. Inosov, A. Leineweber, Xiaoping Yang, J. T. Park, N. B. Christensen, R. Dinnebier, G. L. Sun, Ch. Niedermayer, D. Haug, P. W. Stephens, J. Stahn, O. Khvostikova, C. T. Lin, O. K. Andersen, B. Keimer, and V. Hinkov. Suppression of the structural phase transition and lattice softening in slightly underdoped $\text{Ba}_{1-x}\text{K}_x\text{Fe}_2\text{As}_2$ with electronic phase separation. *Phys. Rev. B*, 79:224503, 2009.
- [22] Z. Deng, X. C. Wang, Q.Q. Liu, S. J. Zhang, Y. X. Lv, J. L. Zhu, R.C. Yu, and C.Q. Jin. A new 111 type iron pnictide superconductor LiFeP . *Euro. Phys. Lett.*, 87:3704, 2009.
- [23] X. C. Wang, Q. Q. Liu, Y. X. Lv, W. B. Gao, L. X. Yang, R. C. Yu, F. Y. Li, and C. Q. Jin. The superconductivity at 18 K in LiFeAs system. *Solid State Commun.*, 148:538, 2008.

- [24] M. J. Pitcher, D. R. Parker, P. Adamson, S. J. C. Herkelrath, A. T. Boothroyd, and S. J. Clarke. Structure and superconductivity of LiFeAs. *Chem. Commun.*, 45:5918, 2008.
- [25] C. W. Chu, F. Chen, M. Gooch, A. M. Guloy, B. Lorenz, B. Lv, K. Sasmal, Z. J. Tang, J. H. Tapp, and Y. Y. Xue. The synthesis and characterization of LiFeAs and NaFeAs. *Physica C*, 469:326, 2009.
- [26] Joshua H. Tapp, Zhongjia Tang, Bing Lv, Kalyan Sasmal, Bernd Lorenz, Paul C. W. Chu, and Arnold M. Guloy. LiFeAs: An intrinsic FeAs-based superconductor with $T_c = 18$ K. *Phys. Rev. B*, 78:060505, 2008.
- [27] Z. Deng, X. C. Wang, Q. Q. Liu, S. J. Zhang, Y. X. Lv, J. L. Zhu, R. C. Yu, and C. Q. Jin. A new “111” type iron pnictide superconductor LiFeP. *Euro. Phys. Lett.*, 87:37004, 2009.
- [28] S. J. Zhang, X. C. Wang, Q. Q. Liu, Y. X. Lv, X. H. Yu, Z. J. Lin, Y. S. Zhao, L. Wang, Y. Ding, H. K. Mao, and C. Q. Jin. Superconductivity at 31 K in the “111”-type iron arsenide superconductor $\text{Na}_{1-x}\text{FeAs}$ induced by pressure. *Euro. Phys. Lett.*, 88:47008, 2009.
- [29] Fong-Chi Hsu, Jiu-Yong Luo, Kuo-Wei Yeh, Ta-Kun Chen, Tzu-Wen Huang, Phillip M. Wu, Yong-Chi Lee, Yi-Lin Huang, Yan-Yi Chu, Der-Chung Yan, and Maw-Kuen Wu. Superconductivity in the PbO-type Structure $\alpha\text{-FeSe}$. *Proc. Natl. Acad. Sci. USA*, 105:14262, 2008.
- [30] Kuo-Wei Yeh, Tzu-Wen Huang, Yi-Lin Huang, Ta-Kun Chen, Fong-Chi Hsu, Phillip M. Wu, Yong-Chi Lee, Yan-Yi Chu, Chi-Liang Chen, Jiu-Yong Luo, Der-Chung Yan, and Maw kuen Wu. Tellurium substitution effect on superconductivity of the α -phase Iron Selenide. *Euro. Phys. Lett.*, 84:37002, 2008.
- [31] B. C. Sales, A. S. Sefat, M. A. McGuire, R. Y. Jin, D. Mandrus, and Y. Mozharivskyj. Bulk superconductivity at 14 K in single crystals of $\text{Fe}_{1+y}\text{Te}_x\text{Se}_{1-x}$. *Phys. Rev. B*, 79:094521, 2009.
- [32] G. F. Chen, Z. G. Chen, J. Dong, W. Z. Hu, G. Li, X. D. Zhang, P. Zheng, J. L. Luo, and N. L. Wang. Electronic properties of single-crystalline $\text{Fe}_{1.05}\text{Te}$ and $\text{Fe}_{1.03}\text{Se}_{0.30}\text{Te}_{0.70}$. *Phys. Rev. B*, 79:140509(R), 2009.
- [33] M. H. Fang, H. M. Pham, B. Qian, T. J. Liu, E. K. Vehstedt, Y. Liu, L. Spinu, and Z. Q. Mao. Superconductivity close to magnetic instability in $\text{Fe}(\text{Se}_{1-x}\text{Te}_x)_{0.82}$. *Phys. Rev. B*, 78:224503, 2008.
- [34] Xiyu Zhu, Fei Han, Gang Mu, Peng Cheng, Bing Shen, Bin Zeng, and Hai-Hu Wen. Transition of stoichiometric $\text{Sr}_2\text{VO}_3\text{FeAs}$ to a superconducting state at 37.2 K. *Phys. Rev. B*, 79:220512, 2009.
- [35] Hiraku Ogino, Yutaka Matsumura, Yukari Katsura, Koichi Ushiyama, Shigeru Horii, Kohji Kishio, and Jun ichi Shimoyama. Superconductivity at 17 K in $(\text{Fe}_2\text{P}_2)(\text{Sr}_4\text{Sc}_2\text{O}_6)$: a new superconducting layered pnictide oxide with a thick perovskite oxide layer. *Supercon. Sci. Tech.*, 22:075008, 2009.

- [36] Jun Zhao, Q. Huang, Clarina de la Cruz, J. W. Lynn, M. D. Lumsden, Z. A. Ren, Jie Yang, Xiaolin Shen, Xiaoli Dong, Zhongxian Zhao, and Pengcheng Dai. Lattice and magnetic structures of PrFeAsO , $\text{PrFeAsO}_{0.85}\text{F}_{0.15}$, and $\text{PrFeAsO}_{0.85}$. *Phys. Rev. B*, 78:132504, 2008.
- [37] C. Lester, Jiun-Haw Chu, J. G. Analytis, S. C. Capelli, A. S. Erickson, C. L. Condon, M. F. Toney, I. R. Fisher, and S. M. Hayden. Neutron scattering study of the interplay between structure and magnetism in $\text{Ba}(\text{Fe}_{1-x}\text{Co}_x)_2\text{As}_2$. *Phys. Rev. B*, 79:144523, 2009.
- [38] Y. Qiu, Wei Bao, Q. Huang, T. Yildirim, J. M. Simmons, M. A. Green, J. W. Lynn, Y. C. Gasparovic, J. Li, T. Wu, G. Wu, and X. H. Chen. Crystal Structure and Antiferromagnetic Order in $\text{NdFeAsO}_{1-x}\text{F}_x$ ($x = 0.0$ and 0.2) Superconducting Compounds from Neutron Diffraction Measurements. *Phys. Rev. Lett.*, 101:257002, 2008.
- [39] Neeraj Kumar, Songxue Chi, Ying Chen, Kumari Gaurav Rana, A. K. Nigam, A. Thamizhavel, William Ratcliff, II, S. K. Dhar, and Jeffrey W. Lynn. Evolution of the bulk properties, structure, magnetic order, and superconductivity with Ni doping in $\text{CaFe}_{2-x}\text{Ni}_x\text{As}_2$. *Phys. Rev. B*, 80:144524, 2009.
- [40] C. de la Cruz, Q. Huang, J. W. Lynn, J. Li, W. Ratcliff, J. L. Zarestzky, H. A. Mook, G. F. Chen, J. L. Luo, N. L. Wang, and P. Dai. Magnetic order close to superconductivity in the iron-based layered $\text{LaO}_{1-x}\text{F}_x\text{FeAs}$ systems. *Nature*, 453:899, 2008.
- [41] Q. Huang, Y. Qiu, Wei Bao, M. A. Green, J. W. Lynn, Y. C. Gasparovic, T. Wu, G. Wu, and X. H. Chen. Neutron-Diffraction Measurements of Magnetic Order and a Structural Transition in the Parent BaFe_2As_2 Compound of FeAs-Based High-Temperature Superconductors. *Phys. Rev. Lett.*, 101:257003, 2008.
- [42] Ying Chen, J. W. Lynn, J. Li, G. Li, G. F. Chen, J. L. Luo, N. L. Wang, Pengcheng Dai, C. de la Cruz, and H. A. Mook. Magnetic order of the iron spins in NdFeAsO . *Phys. Rev. B*, 78:064515, 2008.
- [43] M. D. Johannes and I. I. Mazin. Microscopic origin of magnetism and magnetic interactions in ferropnictides. *Phys. Rev. B*, 79:220510(R), 2009.
- [44] Stephen D. Wilson, Z. Yamani, C. R. Rotundu, B. Freelon, E. Bourret-Courchesne, and R. J. Birgeneau. Neutron diffraction study of the magnetic and structural phase transitions in BaFe_2As_2 . *Phys. Rev. B*, 79:184519, 2009.
- [45] M. Kofu, Y. Qiu, Wei bao, S. H. Lee, S. Chang, T. Wu, G. Wu, and X. H. Chen. Neutron scattering investigation of the magnetic order in single crystalline BaFe_2As_2 . *New J. Phys.*, 11:055001, 2009.
- [46] Jun Zhao, Q. Huang, C. de la Cruz, Shiliang Li, J. W. Lynn, Y. Chen, M. A. Green, G. F. Chen, G. Li, Z. Li, J. L. Luo, N. L. WANG, , and Pengcheng Dai. Structural and magnetic phase diagram of $\text{CeFeAsO}_{1-x}\text{F}_x$ and its relation to high-temperature superconductivity. *Nature Mater.*, 7:953, 2008.

- [47] H. Luetkens, H. H. Klauss, M. Kraken, F. J. Litterst, T. Dellmann, R. Klingeler, C. Hess, R. Khasanov, A. Amato, C. Baines, J. Hamann-Borrero, N. Leps, A. Kondrat, G. Behr, J. Werner, and B. Buechner. The electronic phase diagram of the $\text{LaO}_{1-x}\text{F}_x\text{FeAs}$ superconductor. *Nature Mater.*, 8:305, 2009.
- [48] A. J. Drew, Ch Niedermayer, P. J. Baker, F. L. Pratt, S. J. Blundell, T. Lancaster, R. H. Liu, G. Wu, X. H. Chen, I. Watanabe, V. K. Malik, A. Dubroka, M. Roessle, K. W. Kim, C. Baines, and C. Bernhard. Coexistence of static magnetism and superconductivity in $\text{SmFeAsO}_{1-x}\text{F}_x$ as revealed by muon spin rotation. *Nature Mater.*, 8:310, 2009.
- [49] Marianne Rotter, Michael Pangerl, Marcus Tegel, and Dirk Johrendt. Superconductivity and Crystal Structures of $(\text{Ba}_{1-x}\text{K}_x)\text{Fe}_2\text{As}_2$ ($x = 0 - 1$). *Angew. Chem. Int. Ed.*, 47:7949, 2008.
- [50] H. Chen, Y. Ren, Y. Qiu, Wei bao, R. H. Liu, G. Wu, T. Wu, Y. L. Xie, X. F. Wang, Q. Huang, and X. H. Chen. Coexistence of the spin-density-wave and superconductivity in the $(\text{Ba,K})\text{Fe}_2\text{As}_2$. *Euro. Phys. Lett.*, 85:17006, 2009.
- [51] Lei Fang, Huiqian Luo, Peng Cheng, Zhaosheng Wang, Ying Jia, Gang Mu, Bing Shen, I. I. Mazin, Lei Shan, Cong Ren, and Hai-Hu Wen. Roles of multiband effects and electron-hole asymmetry in the superconductivity and normal-state properties of $\text{Ba}(\text{Fe}_{1-x}\text{Co}_x)_2\text{As}_2$. *Phys. Rev. B*, 80:140508(R), 2009.
- [52] Jiun-Haw Chu, James G. Analytis, Chris Kucharczyk, and Ian R. Fisher. Determination of the phase diagram of the electron-doped superconductor $\text{Ba}(\text{Fe}_{1-x}\text{Co}_x)_2\text{As}_2$. *Phys. Rev. B*, 79:014506, 2009.
- [53] R. Khasanov, M. Bendele, A. Amato, P. Babkevich, A. T. Boothroyd, A. Cervellino, K. Conder, S. N. Gvasaliya, H. Keller, H.-H. Klauss, H. Luetkens, V. Pomjakushin, E. Pomjakushina, and B. Roessli. Coexistence of incommensurate magnetism and superconductivity in $\text{Fe}_{1+y}\text{Se}_x\text{Te}_{1-x}$. *Phys. Rev. B*, 80:140511, 2009.
- [54] T. J. Liu, J. Hu, B. Qian, D. Fobes, Z. Q. Mao, W. Bao, M. Reehuis, S. A. J. Kimber, K. Prokes, S. Matas, D. N. Argyriou, A. Hiess, A. Rotaru, H. Pham, L. Spinu, Y. Qiu, V. Thampy, A. T. Savici, J. A. Rodriguez, and C. Broholm. From $(\pi, 0)$ magnetic order to superconductivity with (π, π) magnetic resonance in $\text{Fe}_{1.02}(\text{Te}_{1-x}\text{Se}_x)$. *Nature Mater.*, 9:716, 2010.
- [55] P. L. Paulose, C. S. Yadav, and K. M. Subhedar. Magnetic phase diagram of $\text{Fe}_{1.1}\text{Te}_{1-x}\text{Se}_x$: A comparative study with the stoichiometric superconducting $\text{FeTe}_{1-x}\text{Se}_x$ system. *Euro. Phys. Lett.*, 90:27011, 2010.
- [56] N. Katayama, S. Ji, D. Louca, S.-H. Lee, M. Fujita, T. J. Sato, J. S. Wen, Z. J. Xu, G. D. Gu, G. Xu, Z. W. Lin, M. Enoki, S. Chang, K. Yamada, and J. M. Tranquada. Investigation of the spin-glass regime between the antiferromagnetic and superconducting phases in $\text{Fe}_{1+y}\text{Se}_x\text{Te}_{1-x}$. *J. Phys. Soc. Jpn.*, 79:113702, 2010.

- [57] Yoshikazu Mizuguchi and Yoshihiko Takano. Review of Fe Chalcogenides as the Simplest Fe-Based Superconductor. *J. Phys. Soc. Jpn.*, 79:102001, 2010.
- [58] C. Dong, H. Wang, Z. Li, J. Chen, H. Q. Yuan, and M. Fang. Revised Phase Diagram for $\text{FeTe}_{1-x}\text{Se}_x$ system with less excess Fe atoms. *arXiv:1012.5188*, 2010.
- [59] Q. Huang, Jun Zhao, J. W. Lynn, G. F. Chen, J. L. Luo, N. L. Wang, and Pengcheng Dai. Doping evolution of antiferromagnetic order and structural distortion in $\text{LaFeAsO}_{1-x}\text{F}_x$. *Phys. Rev. B*, 78:054529, 2008.
- [60] Michael A. McGuire, Andrew D. Christianson, Athena S. Sefat, Brian C. Sales, Mark D. Lumsden, Rongying Jin, E. Andrew Payzant, David Mandrus, Yanbing Luan, Veerle Keppens, Vijayalaksmi Varadarajan, Joseph W. Brill, Raphaël P. Hermann, Moulay T. Sougrati, Fernande Grandjean, and Gary J. Long. Phase transitions in LaFeAsO : Structural, magnetic, elastic, and transport properties, heat capacity and Mössbauer spectra. *Phys. Rev. B*, 78:094517, 2008.
- [61] S. A. Kivelson and H. Yao. Iron-based superconductors: Unity or diversity? *Nature Mater.*, 7:927, 2008.
- [62] I. I. Mazin, D. J. Singh, M. D. Johannes, and M. H. Du. Unconventional Superconductivity with a Sign Reversal in the Order Parameter of $\text{LaFeAsO}_{1-x}\text{F}_x$. *Phys. Rev. Lett.*, 101:057003, 2008.
- [63] Kazuhiko Kuroki, Seiichiro Onari, Ryotaro Arita, Hidetomo Usui, Yukio Tanaka, Hiroshi Kontani, and Hideo Aoki. Unconventional Pairing Originating from the Disconnected Fermi Surfaces of Superconducting $\text{LaFeAsO}_{1-x}\text{F}_x$. *Phys. Rev. Lett.*, 101:087004, 2008.
- [64] Fengjie Ma and Zhong-Yi Lu. Iron-based layered compound LaFeAsO is an antiferromagnetic semimetal. *Phys. Rev. B*, 78:033111, 2008.
- [65] J. Dong, H. J. Zhang, G. Xu, Z. Li, G. Li, W. Z. Hu, D. Wu, G. F. Chen, X. Dai, J. L. Luo, Z. Fang, and N. L. Wang. Competing Orders and Spin-Density-Wave Instability in $\text{La}(\text{O}_{1-x}\text{F}_x)\text{FeAs}$. *Euro. Phys. Lett.*, 83:27006, 2008.
- [66] V. Cvetkovic and Z. Tesanovic. Multiband magnetism and superconductivity in Fe-based compounds. *Euro. Phys. Lett.*, 85:37002, 2009.
- [67] S Graser, T A Maier, P J Hirschfeld, and D J Scalapino. Near-degeneracy of several pairing channels in multiorbital models for the Fe pnictides. *New J. Phys.*, 11:025016, 2009.
- [68] Hisashi Kotegawa, Satoru Masaki, Yoshiki Awai, Hideki Tou, Yoshikazu Mizuguchi, and Yoshihiko Takano. Evidence for Unconventional Superconductivity in Arsenic-Free Iron-Based Superconductor FeSe : A ^{77}Se -NMR Study. *J. Phys. Soc. Jpn.*, 77:113703, 2008.
- [69] C. Fang, H. Yao, W. F. Tsai, J. P. Hu, and S. A. Kivelson. Theory of electron nematic order in LaOFeAs . *Phys. Rev. B*, 77:224509, 2008.
- [70] K Haule and G Kotliar. Coherence–incoherence crossover in the normal state

- of iron oxypnictides and importance of Hund's rule coupling. *New J. Phys.*, 11:025021, 2009.
- [71] Qimiao Si, Elihu Abrahams, Jianhui Dai, and Jian-Xin Zhu. Correlation effects in the iron pnictides. *New J. Phys.*, 11:045001, 2009.
- [72] I. I. Mazin and M. D. Johannes. A key role for unusual spin dynamics in ferropnictides. *Nature Phys.*, 5:141, 2009.
- [73] Su-Peng Kou, Tao Li, and Zheng-yu Weng. Coexistence of itinerant electrons and local moments in iron-based superconductors. *Euro. Phys. Lett.*, 88:17010, 2009.
- [74] Luca de' Medici, Syed R. Hassan, and Massimo Capone. Genesis of coexisting itinerant and localized electrons in Iron Pnictides. *J. Supercond. Nov. Magn.*, 22:535, 2009.
- [75] Wei-Guo Yin, Chi-Cheng Lee, and Wei Ku. Unified Picture for Magnetic Correlations in Iron-Based Superconductors. *Phys. Rev. Lett.*, 105:107004, 2010.
- [76] Ryotaro Arita and Hiroaki Ikeda. Is Fermi-Surface Nesting the Origin of Superconductivity in Iron Pnictides?: A Fluctuation-Exchange-Approximation Study. *J. Phys. Soc. Jpn.*, 78(11):113707, 2009.
- [77] Hiroshi Kontani and Seiichiro Onari. Orbital-Fluctuation-Mediated Superconductivity in Iron Pnictides: Analysis of the Five-Orbital Hubbard-Holstein Model. *Phys. Rev. Lett.*, 104:157001, 2010.
- [78] A. D. Christianson, E. A. Goremychkin, R. Osborn, S. Rosenkranz, M. D. Lumsden, C. D. Malliakas, I. S. Todorov, H. Claus, D. Y. Chung, M. G. Kanatzidis, R. I. Bewley, and T. Guidi. Unconventional superconductivity in $\text{Ba}_{0.6}\text{K}_{0.4}\text{Fe}_2\text{As}_2$ from inelastic neutron scattering. *Nature*, 456:930, 2008.
- [79] M. D. Lumsden, A. D. Christianson, D. Parshall, M. B. Stone, S. E. Nagler, G. J. MacDougall, H. A. Mook, K. Lokshin, T. Egami, D. L. Abernathy, E. A. Goremychkin, R. Osborn, M. A. McGuire, A. S. Sefat, R. Jin, B. C. Sales, and D. Mandrus. Two-dimensional resonant magnetic excitation in $\text{BaFe}_{1.84}\text{Co}_{0.16}\text{As}_2$. *Phys. Rev. Lett.*, 102:107005, 2009.
- [80] Songxue Chi, Astrid Schneidewind, Jun Zhao, Leland W. Harriger, Linjun Li, Yongkang Luo, Guanghan Cao, Zhu'an Xu, Micheal Loewenhaupt, Jiangping Hu, and Pengcheng Dai. Inelastic Neutron-Scattering Measurements of a Three-Dimensional Spin Resonance in the FeAs-Based $\text{BaFe}_{1.9}\text{Ni}_{0.1}\text{As}_2$ Superconductor. *Phys. Rev. Lett.*, 102:107006, 2009.
- [81] Shiliang Li, Ying Chen, Sung Chang, Jeffrey W. Lynn, Linjun Li, Yongkang Luo, Guanghan Cao, Zhu'an Xu, and Pengcheng Dai. Spin gap and magnetic resonance in superconducting $\text{BaFe}_{1.9}\text{Ni}_{0.1}\text{As}_2$. *Phys. Rev. B*, 79:174527, 2009.
- [82] D. S. Inosov, J. T. Park, P. Bourges, D. L. Sun, Y. Sidis, A. Schneidewind, K. Hradil, D. Haug, C. T. Lin, B. Keimer, and V. Hinkov. Normal-State Spin Dynamics and Temperature-Dependent Spin Resonance Energy in an Optimally Doped Iron Arsenide Superconductor. *Nature Phys.*, 6:178, 2010.

- [83] Shin-ichi Shamoto, Motoyuki Ishikado, Andrew D. Christianson, Mark D. Lumsden, Shuichi Wakimoto, Katsuaki Kodama, Akira Iyo, and Masatoshi Arai. Inelastic neutron scattering study of the resonance mode in the optimally doped pnictide superconductor $\text{LaFeAsO}_{0.92}\text{F}_{0.08}$. *Phys. Rev. B*, 82:172508, 2010.
- [84] Yiming Qiu, Wei Bao, Y. Zhao, Collin Broholm, V. Stanev, Z. Tesanovic, Y. C. Gasparovic, S. Chang, Jin Hu, Bin Qian, Minghu Fang, and Zhiqiang Mao. Spin Gap and Resonance at the Nesting Wave Vector in Superconducting $\text{FeSe}_{0.4}\text{Te}_{0.6}$. *Phys. Rev. Lett.*, 103:067008, 2009.
- [85] H. A. Mook, M. D. Lumsden, A. D. Christianson, S. E. Nagler, Brian C. Sales, Rongying Jin, Michael A. McGuire, Athena S. Sefat, D. Mandrus, T. Egami, and Clarina dela Cruz. Unusual Relationship between Magnetism and Superconductivity in $\text{FeTe}_{0.5}\text{Se}_{0.5}$. *Phys. Rev. Lett.*, 104:187002, 2010.
- [86] Jinsheng Wen, Guangyong Xu, Zhijun Xu, Zhi Wei Lin, Qiang Li, Ying Chen, Songxue Chi, Genda Gu, and J. M. Tranquada. Effect of magnetic field on the spin resonance in $\text{FeTe}_{0.5}\text{Se}_{0.5}$ as seen via inelastic neutron scattering. *Phys. Rev. B*, 81:100513(R), 2010.
- [87] Kenji Ishida, Yusuke Nakai, and Hideo Hosono. To What Extent Iron-Pnictide New Superconductors Have Been Clarified: A Progress Report. *J. Phys. Soc. Jpn.*, 78:062001, 2009.
- [88] Hideo Hosono. Layered Iron Pnictide Superconductors: Discovery and Current Status. *J. Phys. Soc. Jpn. Supplement C*, 77:1, 2008.
- [89] Jeffrey W. Lynn and Pengcheng Dai. Neutron Studies of the Iron-based Family of High T_C Magnetic Superconductors. *Physica C*, 469:469, 2009.
- [90] M. D. Lumsden and A. D. Christianson. Magnetism in Fe-based superconductors. *J. Phys.: Conden. Matter*, 22:203203, 2010.
- [91] Hideo Hosono. Two classes of superconductors discovered in our material research: Iron-based high temperature superconductor and electride superconductor. *Physica C*, 469:314, 2009.
- [92] M.K. Wu, F.C. Hsu, K.W. Yeh, T.W. Huang, J.Y. Luo, M.J. Wang, H.H. Chang, T.K. Chen, S.M. Rao, B.H. Mok, C.L. Chen, Y.L. Huang, C.T. Ke, P.M. Wu, A.M. Chang, C.T. Wu, and T.P. Perng. The development of the superconducting PbO-type β -FeSe and related compounds. *Physica C*, 469:340, 2009.
- [93] Paul C. Canfield and Sergey L. Bud'ko. FeAs-Based Superconductivity: A Case Study of the Effects of Transition Metal Doping on BaFe_2As_2 . *Annual Rev. Conden. Matter Phys.*, 1:27, 2010.
- [94] D. C. Johnston. The puzzle of high temperature superconductivity in layered iron pnictides and chalcogenides. *Adv. Phys.*, 59:803, 2010.
- [95] I. Mazin. Superconductivity gets an iron boost. *Nature*, 464:183, 2010.
- [96] Johnpierre Paglione and Richard L. Greene. High-temperature superconductivity in iron-based materials. *Nature Phys.*, 6:645, 2010.

- [97] Jiangan Guo, Shifeng Jin, Gang Wang, Shunchong Wang, Kaixing Zhu, Tingting Zhou, Meng He, and Xiaolong Chen. Superconductivity in the iron selenide $K_x\text{Fe}_2\text{Se}_2$ ($0 \leq x \leq 1.0$). *Phys. Rev. B*, 82:180520, 2010.
- [98] Y. Mizuguchi, H. Takeya, Y. Kawasaki, T. Ozaki, S. Tsuda, T. Yamaguchi, and Y. Takano. Transport properties of the new Fe-based superconductor $K_x\text{Fe}_2\text{Se}_2$ ($T_c = 33$ K). *Appl. Phys. Lett.*, 98:042511, 2011.
- [99] A. F. Wang, J. J. Ying, Y. J. Yan, R. H. Liu, X. G. Luo, Z. Y. Li, X. F. Wang, M. Zhang, G. J. Ye, P. Cheng, Z. J. Xiang, and X. H. Chen. Superconductivity at 32 K in single-crystalline $\text{Rb}_x\text{Fe}_{2-y}\text{Se}_2$. *Phys. Rev. B*, 83:060512, 2011.
- [100] A Krzton-Maziopa, Z Shermadini, E Pomjakushina, V Pomjakushin, M Bendele, A Amato, R Khasanov, H Luetkens, and K Conder. Synthesis and crystal growth of $\text{Cs}_{0.8}(\text{FeSe}_{0.98})_2$: a new iron-based superconductor with $T_c = 27$ K. *J. Phys. Condens. Matter*, 23:052203, 2011.
- [101] Hang-Dong Wang, Chi-Heng Dong, Zu-Juan Li, Qian-Hui Mao, Sha-Sha Zhu, Chun-Mu Feng, H. Q. Yuan, and Ming-Hu Fang. Superconductivity at 32 K and anisotropy in $\text{Tl}_{0.58}\text{Rb}_{0.42}\text{Fe}_{1.72}\text{Se}_2$ crystals. *Euro. Phys. Lett.*, 93:47004, 2011.
- [102] H. Okamoto. The Fe-Se (Iron-Selenium) system. *J. Phase Equilib.*, 12:383, 1991.
- [103] T. M. McQueen, Q. Huang, V. Ksenofontov, C. Felser, Q. Xu, H. Zandbergen, Y. S. Hor, J. Allred, A. J. Williams, D. Qu, J. Checkelsky, N. P. Ong, and R. J. Cava. Extreme sensitivity of superconductivity to stoichiometry in $\text{Fe}_{1+\delta}\text{Se}$. *Phys. Rev. B*, 79:014522, 2009.
- [104] U. Patel, J. Hua, S. H. Yu, S. Avci, Z. L. Xiao, H. Claus, J. Schlueter, V. V. Vlasko-Vlasov, U. Welp, and W. K. Kwok. Growth and superconductivity of FeSe_x crystals. *Appl. Phys. Lett.*, 94:082508, 2009.
- [105] S B Zhang, Y P Sun, X D Zhu, X B Zhu, B S Wang, G Li, H C Lei, X Luo, Z R Yang, W H Song, and J M Dai. Crystal growth and superconductivity of FeSe_x . *Supercond. Sci. Technol.*, 22:015020, 2009.
- [106] Rongwei Hu, Hechang Lei, Milinda Abeykoon, Emil S. Bozin, Simon J. L. Billinge, J. B. Warren, Theo Siegrist, and C. Petrovic. Synthesis, crystal structure, and magnetism of $\beta\text{-Fe}_{1.00(2)}\text{Se}_{1.00(3)}$ single crystals. *Phys. Rev. B*, 83:224502, 2011.
- [107] B. H. Mok, S. M. Rao, M. C. Ling, K. J. Wang, C. T. Ke, P. M. Wu, C. L. Chen, F. C. Hsu, T. W. Huang, J. Y. Luo, D. C. Yan, K. W. Ye, T. B. Wu, A. M. Chang, and M. K. Wu. Growth and Investigation of Crystals of the New Superconductor $\alpha\text{-FeSe}$ from KCl Solutions. *Crystal Growth and Design*, 9(7):3260, 2009.
- [108] H. Okamoto and L. E. Tanner. Fe-Te (Iron-Tellurium). *Binary Alloy Phase Diagrams*, 2:1781, 1990.
- [109] Y. Mizuguchi, K. Deguchi, Y. Kawasaki, T. Ozaki, M. Nagao, S. Tsuda, T. Yamaguchi, and Y. Takano. Superconductivity in oxygen-annealed $\text{FeTe}_{1-x}\text{S}_x$ single crystal. *J. Appl. Phys.*, 109:013914, 2011.

- [110] T. J. Liu, X. Ke, B. Qian, J. Hu, D. Fobes, E. K. Vehstedt, H. Pham, J. H. Yang, M. H. Fang, L. Spinu, P. Schiffer, Y. Liu, and Z. Q. Mao. Charge-carrier localization induced by excess Fe in the superconductor $\text{Fe}_{1+y}\text{Te}_{1-x}\text{Se}_x$. *Phys. Rev. B*, 80:174509, 2009.
- [111] Takashi Noji, Takumi Suzuki, Haruki Abe, Tadashi Adachi, Masatsune Kato, and Yoji Koike. Growth, Annealing Effects on Superconducting and Magnetic Properties, and Anisotropy of $\text{FeSe}_{1-x}\text{Te}_x$ ($0.5 \leq x \leq 1$) Single Crystals. *J. Phys. Soc. Jpn.*, 79:084711, 2010.
- [112] Jinhu Yang, Mami Matsui, Masatomo Kawa, Hiroto Ohta, Chishiro Michioka, Chiheng Dong, Hangdong Wang, Huiqiu Yuan, Minghu Fang, and Kazuyoshi Yoshimura. Magnetic and Superconducting Properties in Single Crystalline $\text{Fe}_{1+\delta}\text{Te}_{1-x}\text{Se}_x$ ($x < 0.50$) System. *J. Phys. Soc. Jpn.*, 79:074704, 2010.
- [113] Jinsheng Wen, Guangyong Xu, Zhijun Xu, Zhi Wei Lin, Qiang Li, W. Ratcliff, Genda Gu, and J. M. Tranquada. Short-range incommensurate magnetic order near the superconducting phase boundary in $\text{Fe}_{1+\delta}\text{Te}_{1-x}\text{Se}_x$. *Phys. Rev. B*, 80:104506, 2009.
- [114] C. C. Homes, A. Akrap, J. S. Wen, Z. J. Xu, Z. W. Lin, Q. Li, and G. D. Gu. Electronic correlations and unusual superconducting response in the optical properties of the iron-chalcogenide $\text{FeTe}_{0.55}\text{Se}_{0.45}$. *Phys. Rev. B*, 81:180508(R), 2010.
- [115] S.-H. Lee, Guangyong Xu, W. Ku, J. S. Wen, C. C. Lee, N. Katayama, Z. J. Xu, S. Ji, Z. W. Lin, G. D. Gu, H.-B. Yang, P. D. Johnson, Z.-H. Pan, T. Valla, M. Fujita, T. J. Sato, S. Chang, K. Yamada, and J. M. Tranquada. Coupling of spin and orbital excitations in the iron-based superconductor $\text{FeTe}_{0.5}\text{Se}_{0.5}$. *Phys. Rev. B*, 81:220502(R), 2010.
- [116] Zhijun Xu, Jinsheng Wen, Guangyong Xu, Qing Jie, Zhiwei Lin, Qiang Li, Songxue Chi, D. K. Singh, Genda Gu, and J. M. Tranquada. Disappearance of static magnetic order and evolution of spin fluctuations in $\text{Fe}_{1+\delta}\text{Se}_x\text{Te}_{1-x}$. *Phys. Rev. B*, 82:104525, 2010.
- [117] I. Pallecchi, G. Lamura, M. Tropeano, M. Putti, R. Viennois, E. Giannini, and D. Van der Marel. Seebeck effect in $\text{Fe}_{1+x}\text{Te}_{1-y}\text{Se}_y$ single crystals. *Phys. Rev. B*, 80:214511, 2009.
- [118] T. Taen, Y. Tsuchiya, Y. Nakajima, and T. Tamegai. Superconductivity at $T_c \sim 14$ K in single-crystalline $\text{FeTe}_{0.61}\text{Se}_{0.39}$. *Phys. Rev. B*, 80:092502, 2009.
- [119] Minghu Fang, Jinhu Yang, F. F. Balakirev, Y. Kohama, J. Singleton, B. Qian, Z. Q. Mao, Hangdong Wang, and H. Q. Yuan. Weak anisotropy of the superconducting upper critical field in $\text{Fe}_{1.11}\text{Te}_{0.6}\text{Se}_{0.4}$ single crystals. *Phys. Rev. B*, 81:020509, 2010.
- [120] Rongwei Hu, Emil S. Bozin, J. B. Warren, and C. Petrovic. Superconductivity, magnetism, and stoichiometry of single crystals of $\text{Fe}_{1+y}(\text{Te}_{1-x}\text{S}_x)_z$. *Phys. Rev. B*, 80:214514, 2009.

- [121] K. W. Yeh, C. T. Ke, T. W. Huang, T. K. Chen, Y. L. Huang, P. M. Wu, and M. K. Wu. Superconducting $\text{FeSe}_{1-x}\text{Te}_x$ Single Crystals Grown by Optical Zone-Melting Technique. *Cryst. Growth Des.*, 9:4847, 2009.
- [122] D. M. Wang, J. B. He, T.-L. Xia, and G. F. Chen. Effect of varying iron content on the transport properties of the potassium-intercalated iron selenide $\text{K}_x\text{Fe}_{2-y}\text{Se}_2$. *Phys. Rev. B*, 83:132502, 2011.
- [123] Hechang Lei and C. Petrovic. Anisotropy in transport and magnetic properties of $\text{K}_{0.64}\text{Fe}_{1.44}\text{Se}_2$. *Phys. Rev. B*, 83:184504, 2011.
- [124] J. J. Ying, X. F. Wang, X. G. Luo, A. F. Wang, M. Zhang, Y. J. Yan, Z. J. Xiang, R. H. Liu, P. Cheng, G. J. Ye, and X. H. Chen. Superconductivity and magnetic properties of single crystals of $\text{K}_{0.75}\text{Fe}_{1.66}\text{Se}_2$ and $\text{Cs}_{0.81}\text{Fe}_{1.61}\text{Se}_2$. *Phys. Rev. B*, 83:212502, 2011.
- [125] Ming-Hu Fang, Hang-Dong Wang, Chi-Heng Dong, Zu-Juan Li, Chun-Mu Feng, Jian Chen, and H. Q. Yuan. Fe-based superconductivity with $T_c = 31$ K bordering an antiferromagnetic insulator in $(\text{Tl,K})\text{Fe}_x\text{Se}_2$. *Euro. Phys. Lett.*, 94:27009, 2011.
- [126] Z. Gao, Y. Qi, L. Wang, C. Yao, D. Wang, X. Zhang, and Y. Ma. Upper fields and critical current density of $\text{K}_{0.58}\text{Fe}_{1.56}\text{Se}_2$ single crystals grown by one step technique. *arXiv:1103.2904*, 2011.
- [127] Jinsheng Wen. *Interplay between magnetism and superconductivity in high-temperature superconductors $\text{La}_{2-x}\text{Ba}_x\text{CuO}_4$ and $\text{Fe}_{1+y}\text{Te}_{1-x}\text{Se}_x$: crystal growth and neutron scattering studies*. PhD thesis, Stony Brook University, 2010.
- [128] Zhijun Xu, Jinsheng Wen, Guangyong Xu, Sujung Han, Qiang Li, J. M. Tranquada, and Genda Gu. unpublished.
- [129] B. Joseph, A. Iadecola, A. Puri, L. Simonelli, Y. Mizuguchi, Y. Takano, and N. L. Saini. Evidence of local structural inhomogeneity in $\text{FeSe}_{1-x}\text{Te}_x$ from extended x-ray absorption fine structure. *Phys. Rev. B*, 82:020502(R), 2010.
- [130] Hefei Hu, J. M. Zuo, J. S. Wen, Z. J. Xu, Z. W. Lin, Q. Li, Genda Gu, W. K. Park, and L. H. Greene. Phase Separation and Chemical Inhomogeneity in the Iron Chalcogenide Superconductor $\text{Fe}_{1+y}\text{Te}_x\text{Se}_{1-x}$. *arXiv:1009.6010*, 2010.
- [131] Xiaobo He, Guorong Li, Jiandi Zhang, A. B. Karki, Rongying Jin, B. C. Sales, A. S. Sefat, M. A. McGuire, D. Mandrus, and E. W. Plummer. Nanoscale chemical phase separation in $\text{FeTe}_{0.55}\text{Se}_{0.45}$ as seen via scanning tunneling spectroscopy. *Phys. Rev. B*, 83:220502, 2011.
- [132] Z. Wang, Y. J. Song, H. L. Shi, Z. W. Wang, Z. Chen, H. F. Tian, G. F. Chen, J. G. Guo, H. X. Yang, and J. Q. Li. Microstructure and ordering of iron vacancies in the superconductor system $\text{K}_y\text{Fe}_x\text{Se}_2$ as seen via transmission electron microscopy. *Phys. Rev. B*, 83:140505, 2011.
- [133] F. Chen, M. Xu, Q. Q. Ge, Y. Zhang, Z. R. Ye, L. X. Yang, J. Jiang, B. P. Xie, R. C. Che, M. Zhang, A. F. Wang, X. H. Chen, D. W. Shen, X. M. Xie, M. H. Jiang, J. P. Hu, and D. L. Feng. Electronic identification of the actual parental

- phase of $K_x\text{Fe}_{2-y}\text{Se}_2$ superconductor and its intrinsic mesoscopic phase separation. *arXiv:1106.3026*, 2011.
- [134] Serena Margadonna, Yasuhiro Takabayashi, Martin T. McDonald, Karolina Kasperkiewicz, Yoshikazu Mizuguchi, Yoshihiko Takano, Andrew N. Fitch, Emmanuelle Suard, and Kosmas Prassides. Crystal structure of the new FeSe_{1-x} superconductor. *Chem. Commun.*, page 5607, 2008.
- [135] E. Pomjakushina, K. Conder, V. Pomjakushin, M. Bendele, and R. Khasanov. Synthesis, crystal structure, and chemical stability of the superconductor FeSe_{1-x} . *Phys. Rev. B*, 80:024517, 2009.
- [136] X. Liu, C.-C. Lee, Z. J. Xu, J. S. Wen, G. Gu, W. Ku, J. M. Tranquada, and J. P. Hill. X-ray diffuse scattering study of local distortions in Fe_{1+x}Te induced by excess Fe. *Phys. Rev. B*, 83:184523, 2011.
- [137] T. M. McQueen, A. J. Williams, P. W. Stephens, J. Tao, Y. Zhu, V. Ksenofontov, F. Casper, C. Felser, and R. J. Cava. Tetragonal-to-Orthorhombic Structural Phase Transition at 90 K in the Superconductor $\text{Fe}_{1.01}\text{Se}$. *Phys. Rev. Lett.*, 103:057002, 2009.
- [138] Wei Bao, Y. Qiu, Q. Huang, M. A. Green, P. Zajdel, M. R. Fitzsimmons, M. Zhernenkov, M. Fang, B. Qian, E. K. Vehstedt, J. Yang, H. M. Pham, L. Spinu, and Z. Q. Mao. Tunable $(\delta\pi, \delta\pi)$ -Type Antiferromagnetic Order in $\alpha\text{-Fe}(\text{Te}, \text{Se})$ Superconductors. *Phys. Rev. Lett.*, 102:247001, 2009.
- [139] Shiliang Li, Clarina de la Cruz, Q. Huang, Y. Chen, J. W. Lynn, Jiangping Hu, Yi-Lin Huang, Fong-Chi Hsu, Kuo-Wei Yeh, Maw kuen Wu, and Pengcheng Dai. First-order magnetic and structural phase transitions in $\text{Fe}_{1+y}\text{Se}_x\text{Te}_{1-x}$. *Phys. Rev. B*, 79:054503, 2009.
- [140] A. Martinelli, A. Palenzona, M. Tropeano, C. Ferdeghini, M. Putti, M. R. Cimberle, T. D. Nguyen, M. Affronte, and C. Ritter. From antiferromagnetism to superconductivity in $\text{Fe}_{1+y}\text{Te}_{1-x}\text{Se}_x$ ($0 \leq x \leq 0.20$): Neutron powder diffraction analysis. *Phys. Rev. B*, 81:094115, 2010.
- [141] Y. Mizuguchi, F. Tomioka, S. Tsuda, T. Yamaguchi, and Y. Takano. Superconductivity in S-substituted FeTe. *Appl. Phys. Lett.*, 94:012503, 2009.
- [142] Y. Mizuguchi, F. Tomioka, S. Tsuda, T. Yamaguchi, and Y. Takano. FeTe as a candidate material for new iron-based superconductor. *Physica C*, 469:1027, 2009.
- [143] Yoshikazu Mizuguchi, Fumiaki Tomioka, Shunsuke Tsuda, Takahide Yamaguchi, and Yoshihiko Takano. Substitution Effects on FeSe Superconductor. *J. Phys. Soc. Jpn.*, 78:074712, 2009.
- [144] Weidong Si, Zhi-Wei Lin, Qing Jie, Wei-Guo Yin, Juan Zhou, Genda Gu, P. D. Johnson, and Qiang Li. Enhanced superconducting transition temperature in $\text{FeSe}_{0.5}\text{Te}_{0.5}$ thin films. *Appl. Phys. Lett.*, 95:052504, 2009.
- [145] Ichiro Tsukada, Masafumi Hanawa, Takanori Akiike, Fuyuki Nabeshima, Yoshinori Imai, Ataru Ichinose, Seiki Komiya, Tatsuo Hikage, Takahiko

- Kawaguchi, Hiroshi Ikuta, and Atsutaka Maeda. Epitaxial Growth of $\text{FeSe}_{0.5}\text{Te}_{0.5}$ Thin Films on CaF_2 Substrates with High Critical Current Density. *Applied Physics Express*, 4:053101, 2011.
- [146] Yoshinori Imai, Ryo Tanaka, Takanori Akiike, Masafumi Hanawa, Ichiro Tsukada, and Atsutaka Maeda. Superconductivity of $\text{FeSe}_{0.5}\text{Te}_{0.5}$ Thin Films Grown by Pulsed Laser Deposition. *Jpn. J. Appl. Phys.*, 49:023101, 2010.
- [147] M. K. Wu, K. W. Yeh, H. C. Hsu, T. W. Huang, T. K. Chen, J. Y. Luo, M. J. Wang, H. H. Chang, C. Ke, M. H. Moh, and S. M. D Rao. The development of the superconducting tetragonal PbO-type FeSe and related compounds. *Physica Status Solidi (B)*, 247:500, 2010.
- [148] Takanori Kida, Takahiro Matsunaga, Masayuki Hagiwara, Yoshikazu Mizuguchi, Yoshihiko Takano, and Koichi Kindo. Upper critical fields of the 11-system iron-chalcogenide superconductor $\text{FeSe}_{0.25}\text{Te}_{0.75}$. *J. Phys. Soc. Jpn.*, 78:113701, 2009.
- [149] C S Yadav and P L Paulose. Upper critical field, lower critical field and critical current density of $\text{FeTe}_{0.60}\text{Se}_{0.40}$ single crystals. *New J. Phys.*, 11:103046, 2009.
- [150] S. Rößler, Dona Cherian, S. Harikrishnan, H. L. Bhat, Suja Elizabeth, J. A. Mydosh, L. H. Tjeng, F. Steglich, and S. Wirth. Disorder-driven electronic localization and phase separation in superconducting $\text{Fe}_{1+y}\text{Te}_{0.5}\text{Se}_{0.5}$ single crystals. *Phys. Rev. B*, 82:144523, 2010.
- [151] M. Bendele, P. Babkevich, S. Katrych, S. N. Gvasaliya, E. Pomjakushina, K. Conder, B. Roessli, A. T. Boothroyd, R. Khasanov, and H. Keller. Tuning the superconducting and magnetic properties of $\text{Fe}_y\text{Se}_{0.25}\text{Te}_{0.75}$ by varying the iron content. *Phys. Rev. B*, 82:212504, 2010.
- [152] E. E. Rodriguez, C. Stock, P. Hsieh, N. Butch, J. Paglione, and M. A. Green. Interstitial Iron Controlled Superconductivity in $\text{Fe}_{1+x}\text{Te}_{0.7}\text{Se}_{0.3}$. *arXiv:1012.0590*, 2010.
- [153] S. Medvedev, T. M. McQueen, I. Trojan, T. Palasyuk, M. I. Erements, R. J. Cava, S. Naghavi, F. Casper, V. Ksenofontov, G. Wortmann, and C. Felser. Electronic and magnetic phase diagram of $\alpha\text{-Fe}_{1.01}\text{Se}$ with superconductivity at 36.7 K under pressure. *Nature Mater.*, 8:630, 2009.
- [154] S. Margadonna, Y. Takabayashi, Y. Ohishi, Y. Mizuguchi, Y. Takano, T. Kagayama, T. Nakagawa, M. Takata, and K. Prassides. Pressure evolution of the low-temperature crystal structure and bonding of the superconductor FeSe ($T_c = 37$ K). *Phys. Rev. B*, 80:064506, 2009.
- [155] Satoru Masaki, Hisashi Kotegawa, Yudai Hara, Hideki Tou, Keizo Murata, Yoshikazu Mizuguchi, and Yoshihiko Takano. Precise Pressure Dependence of the Superconducting Transition Temperature of FeSe: Resistivity and ^{77}Se -NMR Study. *J. Phys. Soc. Jpn.*, 78:063704, 2009.
- [156] V. G. Tissen, E. G. Ponyatovsky, M. V. Nefedova, A. N. Titov, and V. V.

- Fedorenko. Effects of pressure-induced phase transitions on superconductivity in single-crystal $\text{Fe}_{1.02}\text{Se}$. *Phys. Rev. B*, 80:092507, 2009.
- [157] Yoshikazu Mizuguchi, Fumiaki Tomioka, Shunsuke Tsuda, Takahide Yamaguchi, and Yoshihiko Takano. Superconductivity at 27 K in tetragonal FeSe under high pressure. *Appl. Phys. Lett.*, 93:152505, 2008.
- [158] K. Miyoshi, Y. Takaichi, E. Mutou, K. Fujiwara, and J. Takeuchi. Anomalous Pressure Dependence of the Superconducting Transition Temperature in FeSe_{1-x} Studied by DC Magnetic Measurements. *J. Phys. Soc. Jpn.*, 78:093703, 2009.
- [159] Kazumasa Horigane, Nao Takeshita, Chul-Ho Lee, Haruhiro Hiraka, and Kazuyoshi Yamada. First Investigation of Pressure Effects on Transition from Superconductive to Metallic Phase in $\text{FeSe}_{0.5}\text{Te}_{0.5}$. *J. Phys. Soc. Jpn.*, 78:063705, 2009.
- [160] Yoshikazu Mizuguchi, Fumiaki Tomioka, Keita Deguchi, Shunsuke Tsuda, Takahide Yamaguchi, and Yoshihiko Takano. Pressure effects on FeSe family superconductors. *Physica C*, 470:S353, 2010.
- [161] Y Mizuguchi, Y Hara, K Deguchi, S Tsuda, T Yamaguchi, K Takeda, H Kotegawa, H Tou, and Y Takano. Anion height dependence of T_c for the Fe-based superconductor. *Supercond. Sci. Technol.*, 23:054013, 2010.
- [162] Nathalie C. Gresty, Yasuhiro Takabayashi, Alexey Y. Ganin, Martin T. McDonald, John B. Claridge, Duong Giap, Yoshikazu Mizuguchi, Yoshihiko Takano, Tomoko Kagayama, Yasuo Ohishi, Masaki Takata, Matthew J. Rosseinsky, Serena Margadonna, and Kosmas Prassides. Structural Phase Transitions and Superconductivity in $\text{Fe}_{1+\delta}\text{Se}_{0.57}\text{Te}_{0.43}$ at Ambient and Elevated Pressures. *J. Am. Chem. Soc.*, 131:16944, 2009.
- [163] Hironari Okada, Hiroyuki Takahashi, Yoshikazu Mizuguchi, Yoshihiko Takano, and Hiroki Takahashi. Successive Phase Transitions under High Pressure in $\text{FeTe}_{0.92}$. *J. Phys. Soc. Jpn.*, 78:083709, 2009.
- [164] Chao Zhang, Wei Yi, Liling Sun, Xiao-Jia Chen, Russell J. Hemley, Hongkwang Mao, Wei Lu, Xiaoli Dong, Ligang Bai, Jing Liu, Antonio F. Moreira Dos Santos, Jamie J. Molaison, Christopher A. Tulk, Genfu Chen, Nanlin Wang, and Zhongxian Zhao. Pressure-induced lattice collapse in the tetragonal phase of single-crystalline $\text{Fe}_{1.05}\text{Te}$. *Phys. Rev. B*, 80:144519, 2009.
- [165] Y. Han, W. Y. Li, L. X. Cao, X. Y. Wang, B. Xu, B. R. Zhao, Y. Q. Guo, and J. L. Yang. Superconductivity in Iron Telluride Thin Films under Tensile Stress. *Phys. Rev. Lett.*, 104:017003, 2010.
- [166] Evan Lyle Thomas, Winnie Wong-Ng, Daniel Phelan, and Jasmine N. Millican. Thermopower of Co-doped FeSe. *J. Appl. Phys.*, 105:073906, 2009.
- [167] A. J. Williams, T. M. McQueen, V. Ksenofontov, C. Felser, and R. J. Cava. The metal-insulator transition in $\text{Fe}_{1.01-x}\text{Cu}_x\text{Se}$. *J. Phys. Condens. Matter*, 21:305701, 2009.

- [168] Tzu-Wen Huang, Ta-Kun Chen, Kuo-Wei Yeh, Chung-Ting Ke, Chi Liang Chen, Yi-Lin Huang, Fong-Chi Hsu, Maw-Kuen Wu, Phillip M. Wu, Maxim Avdeev, and Andrew J. Studer. Doping-driven structural phase transition and loss of superconductivity in $M_x\text{Fe}_{1-x}\text{Se}_\delta$ ($M = \text{Mn}, \text{Cu}$). *Phys. Rev. B*, 82:104502, 2010.
- [169] S. B. Zhang, H.C. Lei, X.D. Zhu, G. Li, B.S. Wang, L.J. Li, X.B. Zhu, W.H. Song, Z.R. Yang, and Y.P. Sun. Divergency of SDW and structure transition in $\text{Fe}_{1-x}\text{Ni}_x\text{Se}_{0.82}$ superconductors. *Physica C*, 469:1958, 2009.
- [170] D. J. Gawryluk, J. Fink-Finowicki, A. Wisniewski, R. Puzniak, V. Domukhovski, R. Diduszko, M. Kozlowski, and M. Berkowski. Growth conditions, structure, and superconductivity of pure and metal-doped $\text{FeTe}_{1-x}\text{Se}_x$ single crystals. *Supercond. Sci. Tech.*, 24:065011, 2011.
- [171] R. Shipra, H. Takeya, K. Hirata, and A. Sundaresan. Effects of Ni and Co doping on the physical properties of tetragonal $\text{FeSe}_{0.5}\text{Te}_{0.5}$ superconductor. *Physica C*, 470:528, 2010.
- [172] P. Zajdel, M. Zubko, J. Kusz, and M. A. Green. Single crystal growth and structural properties of iron telluride doped with nickel. *Cryst. Res. Technol.*, 45:1316, 2010.
- [173] B. Zeng, B. Shen, G. F. Chen, J. B. He, D. M. Wang, C. H. Li, and H. H. Wen. Nodeless superconductivity of single-crystalline $\text{K}_x\text{Fe}_{2-y}\text{Se}_2$ revealed by the low-temperature specific heat. *Phys. Rev. B*, 83:144511, 2011.
- [174] R. Hu, K. Cho, H. Kim, H. Hodovanets, W. E. Straszheim, M. A. Tanatar, R. Prozorov, S. L. Bud'ko, and P. C. Canfield. Anisotropic magnetism, resistivity, London penetration depth and magneto-optical imaging of superconducting $\text{K}_{0.86}\text{Fe}_{1.84}\text{Se}_2$ single crystals. *Supercon. Sci. Tech.*, 24:065006, 2011.
- [175] Z. Li, X. Ma, H. Pang, and F. Li. Evidence of spin excitation gap in $\text{K}_{0.86}\text{Fe}_{1.73}\text{Se}_2$ superconductor as revealed by Mössbauer spectroscopy. *arXiv:1103.0098*, 2011.
- [176] D. A. Torchetti, M. Fu, D. C. Christensen, K. J. Nelson, T. Imai, H. C. Lei, and C. Petrovic. ^{77}Se NMR investigation of the $\text{K}_x\text{Fe}_{2-y}\text{Se}_2$ high- T_c superconductor ($T_c = 33$ K). *Phys. Rev. B*, 83:104508, 2011.
- [177] R. H. Yuan, T. Dong, G. F. Chen, J. B. He, D. M. Wang, and N. L. Wang. Nanoscale stripe-type phase separation of antiferromagnetic order and superconductivity in $\text{K}_{0.75}\text{Fe}_{1.75}\text{Se}_2$. *arXiv:1102.1381*, 2011.
- [178] E. D. Mun, M. M. Altarawneh, C. H. Mielke, V. S. Zapf, R. Hu, S. L. Bud'ko, and P. C. Canfield. Anisotropic H_{c2} of $\text{K}_{0.8}\text{Fe}_{1.76}\text{Se}_2$ determined up to 60 T. *Phys. Rev. B*, 83:100514, 2011.
- [179] Hisashi Kotegawa, Yudai Hara, Hiroki Nohara, Hideki Tou, Yoshikazu Mizuguchi, Hiroyuki Takeya, and Yoshihiko Takano. Possible Superconducting Symmetry and Magnetic Correlations in $\text{K}_{0.8}\text{Fe}_2\text{Se}_2$: A ^{77}Se -NMR Study. *Phys. Rev. B*, 80:043708, 2011.

- [180] V Yu Pomjakushin, E V Pomjakushina, A Krzton-Maziopa, K Conder, and Z Shermadini. Room temperature antiferromagnetic order in superconducting $X_y\text{Fe}_{2-x}\text{Se}_2$, ($X = \text{Rb}, \text{K}$): a neutron powder diffraction study. *J. Phys. Condens. Matter*, 23:156003, 2011.
- [181] X G Luo, X F Wang, J J Ying, Y J Yan, Z Y Li, M Zhang, A F Wang, P Cheng, Z J Xiang, G J Ye, R H Liu, and X H Chen. Crystal structure, physical properties and superconductivity in $A_x\text{Fe}_2\text{Se}_2$ single crystals. *New J. Phys.*, 13:053011, 2011.
- [182] G. Seyfarth, D. Jaccard, P. Pedrazzini, A. Krzton-Maziopa, E. Pomjakushina, K. Conder, and Z. Shermadini. Pressure cycle of superconducting $\text{Cs}_{0.8}\text{Fe}_2\text{Se}_2$: a transport study. *Solid State Communications*, 151:747, 2011.
- [183] V. Yu. Pomjakushin, D. V. Sheptyakov, E. V. Pomjakushina, A. Krzton-Maziopa, K. Conder, D. Chernyshov, V. Svitlyk, and Z. Shermadini. Iron-vacancy superstructure and possible room-temperature antiferromagnetic order in superconducting $\text{Cs}_y\text{Fe}_{2-x}\text{Se}_2$. *Phys. Rev. B*, 83:144410, 2011.
- [184] R. H. Liu, X. G. Luo, M. Zhang, A. F. Wang, J. J. Ying, X. F. Wang, Y. J. Yan, Z. J. Xiang, P. Cheng, G. J. Ye, Z. Y. Li, and X. H. Chen. Coexistence of superconductivity and antiferromagnetism in single crystals $A_{0.8}\text{Fe}_{2-y}\text{Se}_2$ ($A = \text{K}, \text{Rb}, \text{Cs}, \text{Tl}/\text{K}$ and Tl/Rb): Evidence from magnetization and resistivity. *Euro. Phys. Lett.*, 94:27008, 2011.
- [185] Z. Shermadini, A. Krzton-Maziopa, M. Bendele, R. Khasanov, H. Luetkens, K. Conder, E. Pomjakushina, S. Weyeneth, V. Pomjakushin, O. Bossen, and A. Amato. Coexistence of Magnetism and Superconductivity in the Iron-Based Compound $\text{Cs}_{0.8}(\text{FeSe}_{0.98})_2$. *Phys. Rev. Lett.*, 106:117602, 2011.
- [186] H. Lei, K. Wang, J. B. Warren, and C. Petrovic. Magnetic and superconducting phase diagram of $\text{K}_x\text{Fe}_{2-y}\text{Se}_{2-z}\text{S}_z$ ($0 \leq z \leq 2$). *arXiv:1102.2434*, 2011.
- [187] L. Li, Z. R. Yang, Z. T. Zhang, W. Tong, C. J. Zhang, S. Tan, and Y. H. Zhang. Coexistence of superconductivity and magnetism in $\text{K}_{0.8}\text{Fe}_2\text{Se}_{1.4}\text{S}_{0.4}$. *arXiv:1101.5327*, 2011.
- [188] T. Zhou, X. Chen, J. Guo, G. Wang, X. Lai, S. Wang, S. Jin, and K. Zhu. Quenching of superconductivity by Co doping in $\text{K}_{0.8}\text{Fe}_2\text{Se}_2$. *arXiv:1102.3506*, 2011.
- [189] W. Bao, Q. Huang, G. F. Chen, M. A. Green, D. M. Wang, J. B. He, X. Q. Wang, and Y. Qiu. A Novel Large Moment Antiferromagnetic Order in $\text{K}_{0.8}\text{Fe}_{1.6}\text{Se}_2$ Superconductor. *arXiv:1102.0830*, 2011.
- [190] Kefeng Wang, Hechang Lei, and C. Petrovic. Thermoelectric studies of $\text{K}_x\text{Fe}_{2-y}\text{Se}_2$ indicating a weakly correlated superconductor. *Phys. Rev. B*, 83:174503, 2011.
- [191] Chun-Hong Li, Bing Shen, Fei Han, Xiyu Zhu, and Hai-Hu Wen. Transport properties and anisotropy of $\text{Rb}_{1-x}\text{Fe}_{2-y}\text{Se}_2$ single crystals. *Phys. Rev. B*, 83:184521, 2011.

- [192] D. H. Ryan, W. N. Rowan-Weetaluktuk, J. M. Cadogan, R. Hu, W. E. Straszheim, S. L. Bud'ko, and P. C. Canfield. ^{57}Fe Mössbauer study of magnetic ordering in superconducting $\text{K}_{0.80}\text{Fe}_{1.76}\text{Se}_{2.00}$ single crystals. *Phys. Rev. B*, 83:104526, 2011.
- [193] J J Ying, X F Wang, X G Luo, Z Y Li, Y J Yan, M Zhang, A F Wang, P Cheng, G J Ye, Z J Xiang, R H Liu, and X H Chen. Pressure effect on superconductivity of $A_x\text{Fe}_2\text{Se}_2$ ($A = \text{K}$ and Cs). *New J. Phys.*, 13:033008, 2011.
- [194] Daixiang Mou, Shanyu Liu, Xiaowen Jia, Junfeng He, Yingying Peng, Lin Zhao, Li Yu, Guodong Liu, Shaolong He, Xiaoli Dong, Jun Zhang, Hangdong Wang, Chiheng Dong, Minghu Fang, Xiaoyang Wang, Qinjun Peng, Zhimin Wang, Shenjin Zhang, Feng Yang, Zuyan Xu, Chuangtian Chen, and X. J. Zhou. Distinct Fermi Surface Topology and Nodeless Superconducting Gap in $(\text{Tl}_{0.58}\text{Rb}_{0.42})\text{Fe}_{1.72}\text{Se}_2$ Superconductor. *Phys. Rev. Lett.*, 106:107001, 2011.
- [195] J. Guo, X. Chen, G. Wang, T. Zhou, X. Lai, S. Jin, S. Wang, and K. Zhu. Superconductivity on the verge of Mott localization in ternary iron sulfide. *arXiv:1102.3505*, 2011.
- [196] X.-P. Wang, T. Qian, P. Richard, P. Zhang, J. Dong, H.-D. Wang, C.-H. Dong, M.-H. Fang, and H. Ding. Strong nodeless pairing on separate electron Fermi surface sheets in $(\text{Tl},\text{K})\text{Fe}_{1.78}\text{Se}_2$ probed by ARPES. *Euro. Phys. Lett.*, 93:57001, 2011.
- [197] Long Ma, G. F. Ji, J. Zhang, J. B. He, D. M. Wang, G. F. Chen, Wei Bao, and Weiqiang Yu. Superconducting and normal-state properties of single-crystalline $\text{Tl}_{0.47}\text{Rb}_{0.34}\text{Fe}_{1.63}\text{Se}_2$ as seen via ^{77}Se and ^{87}Rb NMR. *Phys. Rev. B*, 83:174510, 2011.
- [198] Y. Kawasaki, Y. Mizuguchi, K. Deguchi, T. Watanabe, T. Ozaki, S. Tsuda, T. Yamaguchi, H. Takeya, and Y. Takano. Pressure study of the new iron-based superconductor $\text{K}_{0.8}\text{Fe}_2\text{Se}_2$. *arXiv:1101.0896*, 2011.
- [199] J. Guo, L. Sun, C. Zhang, J. Guo, X. Chen, Q. Wu, D. Gu, P. Gao, X. Dai, and Z. Zhao. Correlation between superconductivity and resistance hump in $\text{K}_{0.8}\text{Fe}_{1.7}\text{Se}_2$ single crystal under high pressure. *arXiv:1101.0092*, 2011.
- [200] Xun-Wang Yan, Miao Gao, Zhong-Yi Lu, and Tao Xiang. Electronic Structures and Magnetic Order of Ordered-Fe-Vacancy Ternary Iron Selenides $\text{TlFe}_{1.5}\text{Se}_2$ and $A\text{Fe}_{1.5}\text{Se}_2$ ($A = \text{K}$, Rb , or Cs). *Phys. Rev. Lett.*, 106:087005, 2011.
- [201] Xun-Wang Yan, Miao Gao, Zhong-Yi Lu, and Tao Xiang. Ternary iron selenide $\text{K}_{0.8}\text{Fe}_{1.6}\text{Se}_2$ is an antiferromagnetic semiconductor. *Phys. Rev. B*, 83:233205, 2011.
- [202] I.R. Shein and A.L. Ivanovskii. Electronic structure and Fermi surface of new K intercalated iron selenide superconductor $\text{K}_x\text{Fe}_2\text{Se}_2$. *Phys. Lett. A*, 375:1028, 2011.
- [203] I. A. Nekrasov and M. V. Sadovskii. Electronic Structure, Topological Phase Transitions and Superconductivity in $(\text{K},\text{Cs})_x\text{Fe}_2\text{Se}_2$. *Pisma ZhETF*, 93:182, 2011.

- [204] Cao Chao and Dai Jian-Hui. Electronic Structure of KFe_2Se_2 from First Principles Calculations. *Chin. Phys. Lett.*, 28:057402, 2011.
- [205] Chao Cao and Jianhui Dai. Electronic structure and Mott localization of iron-deficient $\text{TlFe}_{1.5}\text{Se}_2$ with superstructures. *Phys. Rev. B*, 83:193104, 2011.
- [206] Y. Zhang, L. X. Yang, M. Xu, Z. R. Ye, F. Chen, C. He, J. Jiang, B. P. Xie, J. J. Ying, X. F. Wang, X. H. Chen, J. P. Hu, and D. L. Feng. Nodeless superconducting gap in $\text{A}_x\text{Fe}_2\text{Se}_2$ ($\text{A} = \text{K}, \text{Cs}$) revealed by angle-resolved photoemission spectroscopy. *Nature Mater.*, 10:273, 2010.
- [207] T. Qian, X.-P. Wang, W.-C. Jin, P. Zhang, P. Richard, G. Xu, X. Dai, Z. Fang, J.-G. Guo, X.-L. Chen, and H. Ding. Absence of holelike Fermi surface in superconducting $\text{K}_{0.8}\text{Fe}_{1.7}\text{Se}_2$ revealed by Angle-Resolved Photoemission Spectroscopy. *Phys. Rev. Lett.*, 106:187001, 2011.
- [208] Lin Zhao, Daixiang Mou, Shanyu Liu, Xiaowen Jia, Junfeng He, Yingying Peng, Li Yu, Xu Liu, Guodong Liu, Shaolong He, Xiaoli Dong, Jun Zhang, J. B. He, D. M. Wang, G. F. Chen, J. G. Guo, X. L. Chen, Xiaoyang Wang, Qinjun Peng, Zhimin Wang, Shenjin Zhang, Feng Yang, Zuyan Xu, Chuangtian Chen, and X. J. Zhou. Common Fermi Surface Topology and Nodeless Superconducting Gap in $\text{K}_{0.68}\text{Fe}_{1.79}\text{Se}_2$ and $(\text{Tl}_{0.45}\text{K}_{0.34})\text{Fe}_{1.84}\text{Se}_2$ Superconductors Revealed from Angle-Resolved Photoemission Spectroscopy. *Phys. Rev. B*, 83:140508, 2011.
- [209] T. A. Maier, S. Graser, P. J. Hirschfeld, and D. J. Scalapino. d -wave pairing from spin fluctuations in the $\text{K}_x\text{Fe}_{2-y}\text{Se}_2$ superconductors. *Phys. Rev. B*, 83:100515, 2011.
- [210] I. I. Mazin and J. Schmalian. Pairing symmetry and pairing state in ferropnictides: Theoretical overview. *Physica C*, 469:614, 2009.
- [211] Fa Wang, Fan Yang, Miao Gao, Zhong-Yi Lu, Tao Xiang, and Dung-Hai Lee. The electron pairing of $\text{K}_x\text{Fe}_{2-y}\text{Se}_2$. *Euro. Phys. Lett.*, 93:57003, 2011.
- [212] Yi Zhou, Dong-Hui Xu, Fu-Chun Zhang, and Wei-Qiang Chen. Theory for superconductivity in $(\text{Tl},\text{K})\text{Fe}_x\text{Se}_2$ as a doped Mott insulator. *Euro. Phys. Lett.*, 95:17003, 2011.
- [213] Yi-Zhuang You, Fan Yang, Su-Peng Kou, and Zheng-Yu Weng. Phase diagram and a possible unified description of intercalated iron selenide superconductors. *arXiv:1103.1902*, 2011.
- [214] Tetsuro Saito, Seiichiro Onari, and Hiroshi Kontani. Emergence of fully gapped s_{++} -wave and nodal d -wave states mediated by orbital and spin fluctuations in a ten-orbital model of KFe_2Se_2 . *Phys. Rev. B*, 83:140512, 2011.
- [215] Weiqiang Yu, L. Ma, J. B. He, D. M. Wang, T.-L. Xia, G. F. Chen, and Wei Bao. ^{77}Se NMR Study of the Pairing Symmetry and the Spin Dynamics in $\text{K}_y\text{Fe}_{2-x}\text{Se}_2$. *Phys. Rev. Lett.*, 106:197001, 2011.
- [216] Fei Han, Bing Shen, Zhen-Yu Wang, and Hai-Hu Wen. Reversibly tuning the

- insulating and superconducting state in $K_xFe_{2-y}Se_2$ crystals by post-annealing. *arXiv:1103.1347*, 2011.
- [217] W. Bao, G. N. Li, Q. Huang, G. F. Chen, J. B. He, M. A. Green, Y. Qiu, D. M. Wang, and J. L. Luo. Vacancy tuned magnetic high- T_c superconductor $K_xFe_{2-x/2}Se_2$. *arXiv:1102.3674*, 2011.
- [218] Rong Yu, Jian-Xin Zhu, and Qimiao Si. Mott Transition in Modulated Lattices and Parent Insulator of $(K,Tl)_yFe_xSe_2$ Superconductors. *Phys. Rev. Lett.*, 106:186401, 2011.
- [219] C. Fang, B. Xu, P. Dai, T. Xiang, and J. Hu. Magnetic Frustration and Iron-Vacancy Ordering in Iron-Chalcogenide. *arXiv:1103.4599*, 2011.
- [220] Alaska Subedi, Lijun Zhang, David J. Singh, and Mao-Hua Du. Density functional study of FeS, FeSe and FeTe: Electronic structure, magnetism, phonons and superconductivity. *Phys. Rev. B*, 78:134514, 2008.
- [221] Y. Xia, D. Qian, L. Wray, D. Hsieh, G. F. Chen, J. L. Luo, N. L. Wang, and M. Z. Hasan. Fermi Surface Topology and Low-Lying Quasiparticle Dynamics of Parent $Fe_{1+x}Te/Se$ Superconductor. *Phys. Rev. Lett.*, 103:037002, 2009.
- [222] K. Nakayama, T. Sato, P. Richard, T. Kawahara, Y. Sekiba, T. Qian, G. F. Chen, J. L. Luo, N. L. Wang, H. Ding, and T. Takahashi. Angle-Resolved Photoemission Spectroscopy of the Iron-Chalcogenide Superconductor $Fe_{1.03}Te_{0.7}Se_{0.3}$: Strong Coupling Behavior and the Universality of Interband Scattering. *Phys. Rev. Lett.*, 105:197001, 2010.
- [223] D. Fruchart, P. Convert, P. Wolfers, R. Madar, J. P. Senateur, and R. Fruchart. Structure antiferromagnetique de $Fe_{1.125}Te$ accompagnée d'une déformation monoclinique. *Mater. Res. Bull.*, 10:169, 1975.
- [224] Alexander V. Balatsky and David Parker. Not all iron superconductors are the same. *Physics*, 2:59, 2009.
- [225] Myung Joon Han and Sergey Y. Savrasov. Doping Driven $(\pi, 0)$ Nesting and Magnetic Properties of $Fe_{1+x}Te$ Superconductors. *Phys. Rev. Lett.*, 103:067001, 2009.
- [226] Fengjie Ma, Wei Ji, Jiangping Hu, Zhong-Yi Lu, and Tao Xiang. First-Principles Calculations of the Electronic Structure of Tetragonal α -FeTe and α -FeSe Crystals: Evidence for a Bicollinear Antiferromagnetic Order. *Phys. Rev. Lett.*, 102:177003, 2009.
- [227] Ari M. Turner, Fa Wang, and Ashvin Vishwanath. Kinetic magnetism and orbital order in iron telluride. *Phys. Rev. B*, 80:224504, 2009.
- [228] Chen Fang, B. Andrei Bernevig, and Jiangping Hu. Theory of Magnetic Order in $Fe_{1+y}Te_{1-x}Se_x$. *Euro. Phys. Lett.*, 86:67005, 2009.
- [229] Chang-Youn Moon and Hyoung Joon Choi. Chalcogen-Height Dependent Magnetic Interactions and Magnetic Order Switching in $FeSe_xTe_{1-x}$. *Phys. Rev. Lett.*, 104:057003, 2010.

- [230] Igor A. Zaliznyak, Zhijun Xu, John M. Tranquada, Genda Gu, Alexei M. Tsvelik, and Matthew B. Stone. Unconventional temperature enhanced magnetism in iron telluride. *arXiv:1103.5073*, 2011.
- [231] T. Imai, K. Ahilan, F. L. Ning, T. M. McQueen, and R. J. Cava. Why Does Undoped FeSe Become A High T_c Superconductor Under Pressure? *Phys. Rev. Lett.*, 102:177005, 2009.
- [232] M. Bendele, A. Amato, K. Conder, M. Elender, H. Keller, H.-H. Klauss, H. Luetkens, E. Pomjakushina, A. Raselli, and R. Khasanov. Pressure Induced Static Magnetic Order in Superconducting FeSe_{1-x} . *Phys. Rev. Lett.*, 104:087003, 2010.
- [233] H. Sabrowsky, M. Rosenberg, D. Welz, P. Deppe, and W. Schäfer. A neutron and Mössbauer study of TlFe_xS_2 compounds. *J. Magn. Magn. Mater.*, 54-57:1497, 1986.
- [234] Lennart Högström, Agneta Seidel, and Rolf Berger. A Mössbauer study of antiferromagnetic ordering in iron deficient $\text{TlFe}_{2-x}\text{Se}_2$. *J. Magn. Magn. Mater.*, 98:37, 1991.
- [235] J. Bacsá, A. Y. Ganin, Y. Takabayashi, K. E. Christensen, K. Prassides, M. J. Rosseinsky, and J. B. Claridge. Cation vacancy order in the $\text{K}_{0.8+x}\text{Fe}_{1.6-y}\text{Se}_2$ system: Five-fold cell expansion accommodates 20% tetrahedral vacancies. *Chem. Sci.*, 2:1054, 2011.
- [236] C. Cao and J. Dai. Block Spin Ground State and 3-Dimensionality of $(\text{K,Tl})\text{Fe}_{1.6}\text{Se}_2$. *arXiv:1102.1344 (to appear in Phys. Rev. Lett.)*, 2011.
- [237] F. Ye, S. Chi, W. Bao, X. F. Wang, J. J. Ying, X. H. Chen, H. D. Wang, C. H. Dong, and M. Fang. Common Structural and Magnetic Framework in the $\text{A}_2\text{Fe}_4\text{Se}_5$ Superconductors. *arXiv:1102.2882*, 2011.
- [238] B. Shen, B. Zeng, G. F. Chen, J. B. He, D. M. Wang, H. Yang, and H. H. Wen. Intrinsic Percolative Superconductivity in $\text{K}_x\text{Fe}_{2-y}\text{Se}_2$ Single Crystals. *arXiv:1104.2008*, 2011.
- [239] A. Ricci, N. Poccia, G. Campi, B. Joseph, G. Arrighetti, L. Barba, M. Reynolds, M. Burghammer, H. Takeya, Y. Mizuguchi, Y. Takano, M. Colapietro, N. L. Saini, and A. Bianconi. Direct evidence of nanoscale phase separation in the iron chalcogenide superconductor $\text{K}_{0.8}\text{Fe}_{1.6}\text{Se}_2$ from scanning nanofocused x-ray diffraction. *arXiv:1107.0412*, 2011.
- [240] Alessandro Ricci, Nicola Poccia, Bobby Joseph, Gianmichele Arrighetti, Luisa Barba, Jasper Plaisier, Gaetano Campi, Yoshikazu Mizuguchi, Hiroyuki Takeya, Yoshihiko Takano, Naurang Lal Saini, and Antonio Bianconi. Intrinsic phase separation in superconducting $\text{K}_{0.8}\text{Fe}_{1.6}\text{Se}_2$ ($T_c = 31.8$ K) single crystals. *Superconductor Science and Technology*, 24:082002, 2011.
- [241] T. A. Maier and D. J. Scalapino. Theory of neutron scattering as a probe of the superconducting gap in the iron pnictides. *Phys. Rev. B*, 78:020514(R), 2008.

- [242] T. A. Maier, S. Graser, D. J. Scalapino, and P. Hirschfeld. Neutron scattering resonance and the iron-pnictide superconducting gap. *Phys. Rev. B*, 79:134520, 2009.
- [243] Eugene Demler and Shou-Cheng Zhang. Theory of the Resonant Neutron Scattering of High- T_c Superconductors. *Phys. Rev. Lett.*, 75:4126, 1995.
- [244] C. D. Batista, G. Ortiz, and A. V. Balatsky. Unified description of the resonance peak and incommensuration in high- T_c superconductors. *Phys. Rev. B*, 64:172508, 2001.
- [245] I. A. Zaliznyak, Z. Xu, J. M. Tranquada, G. Gu, A. M. Tsvelik, and M. B. Stone. Unconventional temperature enhanced magnetism in iron telluride. *arXiv:1103.5073*, 2011.
- [246] D. N. Argyriou, A. Hiess, A. Akbari, I. Eremin, M. M. Korshunov, Jin Hu, Bin Qian, Zhiqiang Mao, Yiming Qiu, Collin Broholm, and W. Bao. Incommensurate itinerant antiferromagnetic excitations and spin resonance in the $\text{FeTe}_{0.6}\text{Se}_{0.4}$ superconductor. *Phys. Rev. B*, 81:220503, 2010.
- [247] Shiliang Li, Chenglin Zhang, Meng Wang, Hui-qian Luo, Xingye Lu, Enrico Faulhaber, Astrid Schneidewind, Peter Link, Jiangping Hu, Tao Xiang, and Pengcheng Dai. Normal-State Hourglass Dispersion of the Spin Excitations in $\text{FeSe}_x\text{Te}_{1-x}$. *Phys. Rev. Lett.*, 105:157002, 2010.
- [248] P. Babkevich, M. Bendele, A. T. Boothroyd, K. Conder, S. N. Gvasaliya, R. Khasanov, E. Pomjakushina, and B. Roessli. Magnetic excitations of $\text{Fe}_{1+y}\text{Se}_x\text{Te}_{1-x}$ in magnetic and superconductive phases. *J. Phys. Condens. Matter*, 22:142202, 2010.
- [249] M. D. Lumsden, A. D. Christianson, E. A. Goremychkin, S. E. Nagler, H. A. Mook, M. B. Stone, D. L. Abernathy, T. Guidi, G. J. MacDougall, C. De La Cruz, A. S. Sefat, M. A. McGuire, B. C. Sales, and D. Mandrus. Evolution of spin excitations into the superconducting state in $\text{FeTe}_{1-x}\text{Se}_x$. *Nature Phys.*, 6:182, 2010.
- [250] S. O. Diallo, V. P. Antropov, T. G. Perring, C. Broholm, J. J. Pulikkotil, N. Ni, S. L. Bud'ko, P. C. Canfield, A. Kreyssig, A. I. Goldman, and R. J. McQueeney. Itinerant Magnetic Excitations in Antiferromagnetic CaFe_2As_2 . *Phys. Rev. Lett.*, 102:187206, 2009.
- [251] Jun Zhao, D. T. Adroja, Dao-Xin Yao, R. Bewley, Shiliang Li, X. F. Wang, G. Wu, X. H. Chen, Jiangping Hu, and Pengcheng Dai. Spin Waves and Magnetic Exchange Interactions in CaFe_2As_2 . *Nature Phys.*, 5:555, 2009.
- [252] P. Dai, H. A. Mook, G. Aeppli, S. M. Hayden, F. Doğan, J. Yu, Y. Yanagida, H. Takashima, Y. Inaguma, M. Itoh, and T. Nakamura. Resonance as a measure of pairing correlations in the high- T_c superconductor YBCO. *Nature*, 406:965, 2000.

- [253] J. M. Tranquada, C. H. Lee, K. Yamada, Y. S. Lee, L. P. Regnault, and H. M. Rønnow. Evidence for an incommensurate magnetic resonance in $\text{La}_{2-x}\text{Sr}_x\text{CuO}_4$. *Phys. Rev. B*, 69:174507, 2004.
- [254] Jun Zhao, Louis-Pierre Regnault, Chenglin Zhang, Miaoying Wang, Zhengcai Li, Fang Zhou, Zhongxian Zhao, Chen Fang, Jiangping Hu, and Pengcheng Dai. Neutron spin resonance as a probe of the superconducting energy gap of $\text{BaFe}_{1.9}\text{Ni}_{0.1}\text{As}_2$ superconductors. *Phys. Rev. B*, 81:180505, 2010.
- [255] Ph. Bourges, B. Keimer, S. Pailhès, L.P. Regnault, Y. Sidis, and C. Ulrich. The resonant magnetic mode: A common feature of high-Tc superconductors. *Physica C*, 424:45, 2005.
- [256] Wei Bao, A. T. Savici, G. E. Granroth, C. Broholm, K. Habicht, Y. Qiu, Jin Hu, Tijiang Liu, and Z. Q. Mao. A Triplet Resonance in Superconducting $\text{FeSe}_{0.4}\text{Te}_{0.6}$. *arXiv:1002.1617*, 2010.
- [257] S. Li, X. Lu, M. Wang, H.-q. Luo, M. Wang, C. Zhang, E. Faulhaber, L.-P. Regnault, D. Singh, and P. Dai. In-plane magnetic field effect on the neutron spin resonance in optimally doped $\text{FeSe}_{0.4}\text{Te}_{0.6}$ and $\text{BaFe}_{1.9}\text{Ni}_{0.1}\text{As}_2$ superconductors. *arXiv:1105.4923*, 2011.
- [258] O. J. Lipscombe, G. F. Chen, Chen Fang, T. G. Perring, D. L. Abernathy, A. D. Christianson, Takeshi Egami, Nanlin Wang, Jiangping Hu, and Pengcheng Dai. Spin Waves in the $(\pi, 0)$ Magnetically Ordered Iron Chalcogenide $\text{Fe}_{1.05}\text{Te}$. *Phys. Rev. Lett.*, 106:057004, 2011.
- [259] C. Stock, E. E. Rodriguez, M. A. Green, and J. A. Rodriguez-Rivera. Gapped spin fluctuations and interstitial iron in the Fe_{1+x}Te parent compound. *arXiv:1103.1811*, 2011.
- [260] Z. Xu, J. Wen, G. Xu, S. Chi, W. Ku, G. Gu, and J. M. Tranquada. Evidence for local moment magnetism in superconducting $\text{FeTe}_{0.35}\text{Se}_{0.65}$. *arXiv:1012.2300*, 2010.
- [261] M. Wang, C. Fang, D.-X. Yao, G. Tan, L. W. Harriger, Y. Song, T. Netherton, C. Zhang, M. Wang, M. B. Stone, W. Tian, J. Hu, and P. Dai. Spin Waves and magnetic exchange interactions in insulating $\text{Rb}_{0.89}\text{Fe}_{1.58}\text{Se}_2$. *arXiv:1105.4675*, 2011.